

# Automated Pavement Condition Assessment using Unmanned Aerial Vehicles (UAVs) and Convolutional Neural Network (CNN)

by

Vinay K. Chawla

May, 2021

Director of Thesis: Carol Massarra, PhD

Major Department: Construction Management

Assessing pavement condition is extremely essential in any effort to reduce future economic losses and improve the structural reliability and resilience. Data resulting from pavement condition assessment are used as a record of infrastructure performance and as a major component to assess their functionality and reliability. However, pavement condition assessment is challenging because of the cost associated with assessment, safety issues, and the accessibility restrictions, especially after natural hazards. This research aims to develop an automated classification model to rapidly classify pavement distresses. High-resolution aerial images representing alligator and longitudinal cracks are collected for flexible pavements using Unmanned Aerial Vehicle (UAV) around East Carolina University (ECU) campus. The image classification model is developed using Convolutional Neural Network (CNN), a deep learning approach. The results of the developed model indicate an accuracy of 96.7% in classifying the two categories of pavement distress. The developed model was further tested on a set of test images yielding a prediction accuracy of 90%. The methodology behind the developed model will help to reduce the need for on-site presence, increase safety, and assist emergency response managers in deciding the safest route to take after hurricane events. Additionally, application of the model will enable transportation engineers in rapidly assessing the pavement damage, aid in making quick decisions for road rehabilitation and recovery and devise a restoration or repair plan.



Automated Pavement Condition Assessment using Unmanned Aerial Vehicles (UAVs) and  
Convolutional Neural Network (CNN)

A Thesis

Presented to The Faculty of the Department of Construction Management

East Carolina University

In Partial Fulfillment of the Requirements for the Degree

Master of Science in Construction Management

by

Vinay K. Chawla

May, 2021

© Vinay K. Chawla, 2021

Automated Pavement Condition Assessment using Unmanned Aerial Vehicles (UAVs) and  
Convolutional Neural Network (CNN)

by

Vinay K. Chawla

APPROVED BY:

DIRECTOR OF  
THESIS:

\_\_\_\_\_  
Carol Massarra, PhD

COMMITTEE MEMBER:

\_\_\_\_\_  
Amin Akhnoukh, PhD

COMMITTEE MEMBER:

\_\_\_\_\_  
Zhen Zhu, PhD

COMMITTEE MEMBER:

\_\_\_\_\_  
Husam Sadek, PhD

CHAIR OF THE DEPARTMENT  
OF CONSTRUCTION MANAGEMENT:

\_\_\_\_\_  
George Wang, PhD

DEAN OF THE GRADUATE SCHOOL:

\_\_\_\_\_  
Paul J. Gemperline, PhD

## TABLE OF CONTENTS

LIST OF TABLES .....	VIII
LIST OF FIGURES .....	XII
CHAPTER 1: INTRODUCTION .....	1
1.1 Problem Statement.....	4
1.2 Goal and Objectives.....	4
1.3 Study Limitation .....	5
1.4 Organization of the Thesis.....	5
CHAPTER 2: LITERATURE REVIEW .....	6
2.1 Introduction .....	6
2.2 Types of Pavement Distresses .....	7
2.3 Pavement Condition Assessment.....	9
2.3.1 Pavement Condition Assessment Methods.....	9
2.4 Comparison of the Manual and Automated Pavement Assessment Methods .....	11
2.5 Commercial Applications of Unmanned Aerial Vehicles (UAVs) in Different Fields...	13
2.6 Automated Pavement Assessment Using Unmanned Aerial Vehicles (UAVs).....	15
2.7 Image Classification for Pavement Condition Assessment .....	18
CHAPTER 3: METHODOLOGY .....	23
3.1 Introduction .....	23
3.2 Definitions .....	23

3.3 Rapid Pavement Condition Assessment Methodology .....	25
3.3.1 Data Collection using UAV .....	26
3.3.2 Pavement Distress Classification Model .....	27
3.3.2.1 Feature Extraction .....	28
3.3.2.2 Classification .....	32
3.3.2.3 AlexNet Conventional Neural Network (CNN).....	33
3.3.2.4 Model Training.....	34
3.3.2.5 Model Validation.....	36
3.3.3 Model Testing .....	36
CHAPTER 4: RESULTS .....	37
4.1 Pavement Distress Classification Model .....	37
4.2 Model Validation .....	39
4.3 Model Testing.....	40
CHAPTER 5: CONCLUSIONS AND RECOMMENDATIONS .....	43
5.1 Conclusions .....	43
5.2 Recommendations and Future Research .....	44
REFERENCES .....	45
APPENDIX.....	52
Flexible Pavement Distresses .....	52
Rigid Pavement Distresses .....	60

## LIST OF TABLES

1. Table 2.1: Relevant Studies Reviewed in the Literature on Image Classification..... 19
2. Table 3.1: Pavement Distress Categories and Frequency of Collected Data for Training and Validation.....34

## LIST OF FIGURES

1. Figure 2.1: Types of Pavement Distresses for Flexible and Rigid Pavements .....	7
2. Figure 2.2: Alligator Cracking in Flexible Pavements .....	8
3. Figure 2.3: Longitudinal Cracking in Flexible Pavements .....	8
4. Figure 2.4: Methods used for Pavement Condition Assessment .....	10
5. Figure 2.5: Comparison of the Traditional and Automated Pavement Assessment Methods Based on Time, Manpower, Cost, and Subjectivity of Evaluation .....	13
6. Figure 3.1: Research Methodology Roadmap.....	25
7. Figure 3.2: Locations of Surveyed Streets with Pavement Distresses on ECU Campus..	26
8. Figure 3.3: DJI Mavic Mini Used for Data Collection .....	27
9. Figure 3.4: Architecture of Conventional Neural Network (CNN) .....	28
10. Figure 3.5: Convolution Operation of Conventional Neural Network (CNN) .....	30
11. Figure 3.6: Pooling Operation of Conventional Neural Network (CNN).....	31
12. Figure 3.7: Layers Involved in the Classification Part of Conventional Neural Network (CNN) .....	33
13. Figure 4.1: Pavement Distress (Alligator and Longitudinal Cracks) Classification Process using CNN.....	38
14. Figure 4.2: Array of Random Images of Pavement Distress used for Model Training ....	38
15. Figure 4.3: Training Process Indicating Accuracy and Loss during Model Training .....	39
16. Figure 4.4: Model Validation Confusion Matrix .....	40
17. Figure 4.5: Model Testing (Correctly Classified Images from the Model) .....	41
18. Figure 4.6: Model Testing (Misclassified Image from the Model) .....	41
19. Figure 4.7: Model Testing Confusion Matrix .....	42
20. Figure A1: Alligator Cracking in Flexible Pavements.....	52

21. Figure A2: Block Cracking in Flexible Pavements .....	53
22. Figure A3: Edge Cracking in Flexible Pavements.....	54
23. Figure A4: Longitudinal Cracking in Flexible Pavements .....	54
24. Figure A5: Reflection Cracking in Flexible Pavements .....	55
25. Figure A6: Transverse Cracking in Flexible Pavements .....	55
26. Figure A7: Patching (a) and Potholes (b) in Flexible Pavements.....	56
27. Figure A8: Surface Defects; Rutting (a) and Shoving (b) in Flexible Pavements.....	57
28. Figure A9: Surface Deformations; Bleeding (a), Polished Aggregate (b), and Raveling (c) in Flexible Pavements.....	58
29. Figure A10: Miscellaneous Distresses; Lane-to-Shoulder Dropoff (a) and Water Bleeding and Pumping in Flexible Pavements.....	59
30. Figure A11: Corner Breaks in Rigid Pavements.....	60
31. Figure A12: Durability “D” Cracking in Rigid Pavements .....	61
32. Figure A13: Longitudinal Cracking in Rigid Pavements .....	61
33. Figure A14: Transverse Cracking in Rigid Pavements.....	62
34. Figure A15: Joint Seal Damage in Rigid Pavements.....	63
35. Figure A16: Spalling of Longitudinal Joints in Rigid Pavements .....	63
36. Figure A17: Spalling of Transverse Joints in Rigid Pavements .....	64
37. Figure A18: Map Cracking (a) and Scaling (b) in Rigid Pavements.....	64
38. Figure A19: Polished Aggregate in Rigid Pavements .....	65
39. Figure A20: Popouts in Rigid Pavements.....	65
40. Figure A21: Blowups in Rigid Pavements .....	66
41. Figure A22: Faulting of Transverse Joints and Cracks in Rigid Pavements .....	66

42. Figure A23: Lane-to-Shoulder Dropoff in Rigid Pavements.....	67
43. Figure A24: Lane-to-Shoulder Separation in Rigid Pavements .....	67
44. Figure A25: Patching in Flexible Pavements.....	68
45. Figure A26: Water Bleeding and Pumping in Rigid Pavements .....	68

## **CHAPTER 1: INTRODUCTION**

Transportation, more importantly road networks, are significant components of infrastructure, which greatly impact the economic and social well-being of a region as people heavily depend on them for their daily activities. Therefore, timely maintenance is critical for their safe and viable operation. Recently, there has been a significant increase in the damage and failure to roads in the coastal communities because of the increase in the frequency and severity of the coastal storms (e.g., hurricanes). Asphalt pavements are an important part of the transportation networks and acquiring critical information on the damages endured by these pavements is essential. This information will help gain knowledge about the underlying physical phenomena, examine the impact of natural hazards on the pavement, effectively assess and mitigate the damage, determine the need for external assistance (Lindell et al., 2003), and aid in rehabilitation and alternative hazard management practices. However, pavement condition assessment is a very challenging process because it is expensive, protracted, and laborious, especially after hurricane events, when access to the disaster struck area is restricted (Morton et al., 2011).

Ground-based traditional approaches for pavement condition assessment mainly rely on expert human visual inspection and observational information along with testing using specialized equipment and personnel to perform the tests (Aksamit et al., 2011). Other instruments such as pavement sensors are also used to monitor the health and performance of pavements (Weinmann et al., 2004). These techniques are labor-intensive and time-consuming, and sometimes require both field and laboratory testing, which at times, cause further damage to the pavements.

In contrast to ground-based traditional approaches, Unmanned Aerial Vehicles (UAVs) or drones have proven to aid in rapid data collection through aerial reconnaissance, provide emergency responses and humanitarian relief, and facilitate aerial monitoring and damage evaluation (Estrada et al., 2019; Restas, 2015), especially for inaccessible areas, where it is difficult

to assess damage (Floreano et al., 2015). The employment of UAVs, as opposed to other aerial imagery such as satellite and standard aviation alternatives, provides operational and economic benefits (Adams et al., 2010; Ezequiel et al., 2014). With researchers focusing on developing low-cost methodologies for disaster assessment using UAVs, damage assessors are encouraged to invest in using UAVs to aid in data collection and damage assessment (Branco et al., 2015). In addition to their efficiency and economy, UAVs unlike manned aircrafts, provide flexibility and maneuverability to capture the necessary data (i.e. high-quality aerial images), without risking personal safety to visually inspect the damaged area in a relatively lesser time period (Erdelj et al., 2017; Luppicini et al., 2016).

Although UAVs have several advantages, there are certain limitations and restrictions on its usage. Adverse weather conditions such as strong winds and rains pose risks to their operation making the flight unstable (High et al., 2019). UAV flights require maintaining a constant visual line of sight between them and the operator to avoid accidents when the UAV encounters Global Position System (GPS) signal losses, especially when flown under a bridge or is swayed by strong winds. Furthermore, UAV operators require licenses and permissions from the Federal Aviation Authority (FAA) (Canis, 2015; Wells et al., 2017). Commercially, the use of UAVs is still contended as it threatens the safety, security, and privacy of people. However, their ability to rapidly collect data and then analyze the digital imagery through image classification techniques cannot be ignored (Rao et al., 2016) and are needed to aid in disaster management and mitigation, especially in coastal communities.

Image classification, which involves extracting information from a digital image, is considered an important part of digital image analysis, and is receiving attention for its potential to rapidly assess condition of structures (e.g., pavements, buildings, bridges) through automated

techniques and improve the quality of damage assessment by reducing subjectivity of information. Several machine and deep learning algorithms such as Support Vector Machine (SVM), Maximum Likelihood Classifier (MLC), Random Forest Classifier (RFC), Deep Neural Networks (DNNs) and Convolutional Neural Networks (CNNs) have been widely used for performing image classification to detect and predict pavement distresses. Among these approaches, CNNs, which stem from the field of deep learning, provide the advantage of reducing the work of pre-preparing images such as feature extraction and format conversion before inputting the images for training and automatically learns the features from the input images, in addition to attaining a higher performance accuracy (Yokoyama et al., 2017). CNNs comprise of a deep network architecture with several hidden layers (Xie et al., 2017) and classify images by perceiving information from the raw input data and then learning from the features of these data.

The advancement in technology and computer vision has made several progresses to reduce human effort in various fields, including civil infrastructure, creating possibilities for automatic pavement distress detection and classification. Hence, to rapidly identify and classify pavement distresses, novel non-traditional pavement condition assessment methods that use aerial images and are based on machine or deep learning classification algorithms are needed to be developed. This study proposes an approach for rapid pavement condition assessment using aerial images obtained from UAVs and an image classification model based on a CNN. The identification of pavement distresses involves acquiring aerial images of the impaired pavements through UAVs and then using a CNN model to classify the pavement distress. The image classification involves training a CNN model based on a dataset containing the images for the pavement distresses and then validating the predicted results for accuracy. The algorithm will then be applied to the test images to identify and classify the pavement distress in for a new dataset.

## **1.1 Problem Statement**

The traditional approaches of pavement assessment are labor intensive, time consuming, and unsafe. The use of UAVs for aerial surveys has significantly reduced both time and labor requirements and made it safer and easier to capture data, while the employment of image classification models has provided rapid analysis and accurate prediction for pavement distresses. Therefore, in order to better understand pavement performance and to rapidly classify pavement distresses, nontraditional pavement assessment methods based on deep learning classification algorithms are needed.

## **1.2 Goal and Objectives**

The main goal of this research is to better understand the performance of pavements and bring an improvement in the pavement assessment methods by developing a procedure that enables rapid pavement condition assessment. As a step towards achieving this goal, the following tasks are undertaken:

1. Examine existing literature to identify pavement condition assessment and image classification practices and determine remaining gaps in existing practices.
2. Collect high resolution aerial images for pavement structures using Unmanned Aerial Vehicle (UAV).
3. Classify pavement distress based on the aerial images collected from objective 2 through the development of deep learning image classification model.

The research calls attention to the following research questions:

- How can UAVs be efficiently used for the pavement distress surveys and collection of aerial imagery?
- What are the implications of deep learning in rapid pavement conditions assessment?

### **1.3 Study Limitation**

This study is limited to the assessment of flexible pavements with two types of pavement distresses, which are alligator and longitudinal cracks. The dataset used to develop the classification model is limited to data resulting from aerial images captured using a UAV around ECU campus. Although the classification model is developed for a specific type and distresses of pavement, the underlying development of the classification model is applicable to other type of pavements (e.g., concrete decks) and distresses (e.g., joint spalling, faulting, cracking).

### **1.4 Organization of the Thesis**

This thesis is divided into five chapters: (1) Introduction; (2) Literature Review; (3) Methodology; (4) Results; and (5) Conclusions, and Recommendations. Chapter 2 provides a literature review of the types of pavement distress, the existing pavement condition assessment methods, and the use of UAVs in pavement monitoring and distress identification along with studies on CNN and its applications in image classification. Chapter 3 outlines the data collection and the methodology used in developing a model for pavement defects classification. Chapter 4 presents the results of the classification model. Chapter 5 provides the overall conclusions, discussions, and recommendations resulting from this research.

## **CHAPTER 2: LITERATURE REVIEW**

### **2.1 Introduction**

Pavement condition assessment and resulting data is an essential part of the pavement management systems as critical information is acquired on the stability and functionality of the pavements to provide timely maintenance, prevent accidents, and ensure user safety (Shiyab, 2007). This information becomes more critical after natural hazard events (e.g., hurricane) as pavement structures have become more vulnerable to damage from flooding induced by hurricane. Increases in flood frequency results in additional damages and loss to pavement. The traditional methods for pavement condition assessment are based on manual inspection, involving physical observations and measurements for the road networks, and testing and recording the data on site, which is time and labor-intensive, requires resources and equipment, and at times unsafe (Coenen et al., 2017; Schnebele et al., 2015). On the other hand, automated assessment approaches can potentially reduce the extensive work of the manual methods and increase cost-effectiveness, efficiency, and safety for pavement condition assessment. These approaches are based on image classification techniques (e.g., deep learning) and use aerial and high-resolution images.

Within the context of the thesis, the second section of this chapter provides a review of the types of pavement distress for flexible rigid pavements; the third section focuses on pavement condition assessment methods; the fourth section provides a comparison between the traditional and non-traditional pavement condition assessment approaches; the fifth section discusses the commercial use of the Unmanned Aerial Vehicles (UAVs); the sixth section describes the automated pavement condition assessment through UAVs, the focus of this thesis ; and the seventh section outlines image classification approaches (e.g., Support Vector Machine (SVM), Convolutional Neural Network (CNN), where CNN is the focus of this research.

## 2.2 Types of Pavement Distresses

Pavement distress is a disfigurement of pavement surfaces due to the combined effect of several factors such as traffic loading, environmental conditions, design, and material failure (Nasir et al., 2018). Based on the type of pavement (i.e., flexible, or rigid), distresses are broadly classified into five categories for flexible pavement and four categories for rigid pavement (Miller et al., 2003). The categories for flexible pavement distresses are cracking, patching and potholes, surface defects, surface deformations, and miscellaneous distresses. The categories for rigid pavements are cracking, joint deficiencies, surface defects, and miscellaneous distresses. There are some similar distresses for both flexible and rigid pavements, however, their characteristics differ because of the difference in material for both pavement types. For example, in the cracking group (i.e., longitudinal and transverse cracking), in the surface defects group (i.e., polished aggregate), and in the miscellaneous distresses group (i.e., lane-to-shoulder dropoff and water bleeding and pumping). In addition, there is patch/patch deterioration which is a distress occurring in both flexible and rigid pavements but is considered in patching and potholes distress group for flexible pavements and in miscellaneous distress group for rigid pavements. The distress types for flexible and rigid pavements are summarized in (Figure 2.1) and are illustrated in detail in the Appendix.

Flexible Pavement Distresses		Rigid Pavement Distresses	
<u>Cracking</u>	<ul style="list-style-type: none"> <li>• Fatigue Cracking</li> <li>• Block Cracking</li> <li>• Edge Cracking</li> <li>• Longitudinal Cracking (Wheel Path and Non-Wheel Path)</li> <li>• Reflection Cracking at Joints</li> <li>• Transverse Cracking</li> </ul>	<u>Cracking</u>	<ul style="list-style-type: none"> <li>• Corner Breaks</li> <li>• Durability Cracking (“D” Cracking)</li> <li>• Longitudinal Cracking</li> <li>• Transverse Cracking</li> </ul>
<u>Patching and Potholes</u>	<ul style="list-style-type: none"> <li>• Patch / Patch Deterioration</li> <li>• Potholes</li> </ul>	<u>Joint Deficiencies</u>	<ul style="list-style-type: none"> <li>• Joint Seal Damage (Transverse and Longitudinal)</li> <li>• Spalling of Longitudinal Joints</li> <li>• Spalling of Transverse Joints</li> </ul>
<u>Surface Deformation</u>	<ul style="list-style-type: none"> <li>• Rutting</li> <li>• Shoving</li> </ul>	<u>Surface Defects</u>	<ul style="list-style-type: none"> <li>• Map Cracking and Scaling</li> <li>• Polished Aggregate</li> <li>• Popouts</li> </ul>
<u>Surface Defects</u>	<ul style="list-style-type: none"> <li>• Bleeding</li> <li>• Polished Aggregate</li> <li>• Raveling</li> </ul>	<u>Miscellaneous Distresses</u>	<ul style="list-style-type: none"> <li>• Blowups</li> <li>• Faulting of Transverse Joints</li> <li>• Lane-to-Shoulder Dropoff</li> <li>• Lane-to-Shoulder Separation</li> <li>• Patch/Patch Deterioration</li> <li>• Water Bleeding and Pumping</li> </ul>
<u>Miscellaneous Distresses</u>	<ul style="list-style-type: none"> <li>• Lane-to-Shoulder Dropoff</li> <li>• Water Bleeding and Pumping</li> </ul>		

Figure 2.1: Types of Pavement Distresses for Flexible and Rigid Pavements

This thesis focuses on two types of flexible pavements distresses (i.e., alligator and longitudinal cracking). Alligator (fatigue) cracking is a consequence of repeated traffic loading, appearing in the form of a series of interconnected cracks (fatigue failure), a pattern resembling the skin of an alligator (Figure 2.2).



Figure 2.2: Alligator Cracking in Flexible Pavements

Longitudinal cracking can either be wheel path or non-wheel path and appears lengthwise along the centerline of the pavement (Figure 2.3). The longitudinal cracks eventually turn into alligator cracking under repeated traffic loading.



Figure 2.3: Longitudinal Cracking in Flexible Pavements

## 2.3 Pavement Condition Assessment

Pavement condition assessment is essential to understand the performance and behavior of pavements and to identify the needed maintenance and repair works. Constant maintenance of pavements is crucial as the pavements deteriorate under repeated traffic loading and environmental conditions. Data resulting from pavement condition assessment may be used in Pavement Management System (PMS) to aid in planning the repair and maintenance works for optimum functioning of pavements (Karim et al., 2016), analyze and project pavement condition, and make repair and maintenance decisions (Pierce et al., 2013). Following are some of the uses of pavement condition data:

- Identifying current condition of pavements
- Establishing models for predicted pavement deterioration
- Projecting future conditions
- Preparing and prioritizing annual and multi-year work programs
- Developing treatment recommendations, timing, and cost
- Allocating resources between regions and/or assets
- Analyzing the impacts of various budget and treatment scenarios
- Analyzing performance of different pavement designs and/or materials

### 2.3.1 Pavement Condition Assessment Methods

Pavement condition assessment methods are broadly categorized into manual and automated techniques (Figure 2.4), where automated techniques include semi and fully techniques. Manual condition assessment is carried out manually by an expert inspector by visually observing the pavements and recording the surface distresses, resulting in the subjective evaluation of pavements. The pavements are evaluated by walking alongside it or travelling at a slow speed and

may be limited to certain segments or spans of the pavement. The quantitative information such as the length, width, and depth of distresses are measured in the field and documented on paper, computer, or hand-held devices (Pierce et al., 2013). Consequently, it is expensive, labor-intensive, and time-consuming to survey roads and obtain condition data for pavement evaluation, producing inconsistent results. In addition, the assessors are exposed to unsafe working conditions, especially on highways (Zakeri et al., 2017).

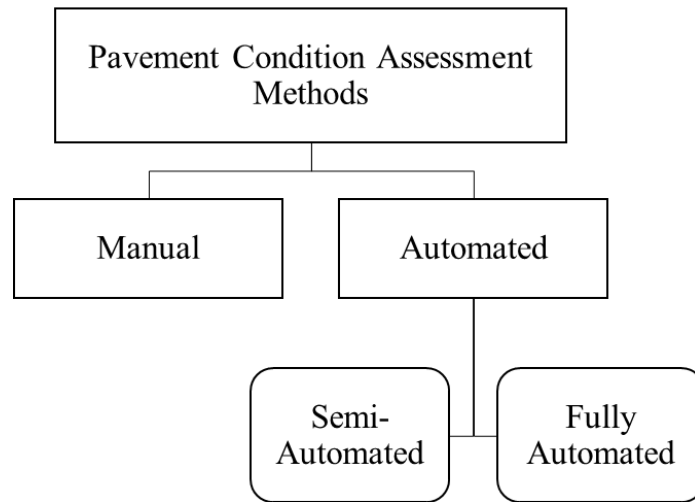


Figure 2.4: Methods used for Pavement Condition Assessment

Over the years, researchers have focused their efforts to innovate and automate the pavement assessment and distress identification and classification processes, in an attempt to reduce time, effort, and subjectivity and provide a rapid pavement condition assessment and produce efficient data for qualitative and quantitative pavement evaluation (Ragnoli et al., 2018). Automated condition assessment uses specialized equipment such as a van equipped cameras, computers, lasers to gather pavement condition data in the form of digital images and videos. The data includes both the longitudinal and transverse profiles of the pavements and is processed through either semi-automated or fully automated means for the condition assessment. In a semi-automated processing, the pavement images are reviewed by human experts to gauge the distresses and

computer software are employed for displaying images and recording distresses. Whereas, in a fully automated processing approach, computer vision and image classification algorithms are used for the identification and classification of distresses (Pierce et al., 2013).

## **2.4 Comparison of the Manual and Automated Pavement Assessment Methods**

Pavement condition assessment is a crucial part of the pavement management system to maintain user comfort and safety for the pavements. Therefore, several state and federal highway agencies (e.g., Federal Highway Administration (FHWA), State Departments of Transportation (DOT), American Society for Testing and Materials (ASTM)) have developed distress identification manuals to identify the type, extent, and severity of distresses. Pavement management for the most part, depend on the identification of pavement surface distress and recording the information based on the pavement evaluation guidelines provided by these manuals for the maintenance and rehabilitation. For many years, the state and federal highway agencies have relied on manual observations of their experts and engineers and their visual inspection of the surface distresses, which were then reported and then documented taking into account the information from the principal manuals. This manual approach was found to be subjective as the results varied with the experience of the personnel inspecting the pavements. The data collection and reporting also prolonged for longer periods, because physical presence on site is required to visually observe the pavement condition, resulting in smaller amounts of data being collected at a given time, which in turn, results in higher resource requirements. Moreover, the traffic and environmental conditions also slowed the process and risking the safety of inspectors. (Attoh-Okine et al., 2013; Cafiso et al., 2006).

With the evolution in technology, newer methods began to be developed for performing the pavement evaluation and collection of data. These methods were established using digital

techniques such as digital cameras, UAVs, for obtaining the pavement data in field and processing them using computer applications. The aim was to automate the pavement condition assessment process and make it less time consuming by covering larger areas and increasing the amount of data collected at a given time. In addition, the image recognition and computer vision tools make the automated pavement assessment more objective as the distress identification is standardized, requiring lesser manpower and cost. It also increases the safety of personnel as the time required in the field is reduced and the data is gathered without physical presence on pavements, as well as the processing takes place in the office through the digital images rather than visual inspection on the field. (Attoh-Okine et al., 2013; Cafiso et al., 2006).

Even though, the automated surveys have been widely adopted because of their resource effectiveness and safety, many agencies still perform the manual inspection for the assessment of pavement (Pierce et al., 2013). Studies have indicated that in most cases, the results from automated surveys are identical to the manual surveys (Coenen et al., 2017; Lekshmipathy et al., 2020; Oliveira et al., 2014; Ragnoli et al., 2018; Tighe et al., 2008) and reduce the time, cost, labor, and subjectivity for the pavement condition assessment (Figure 2.5).

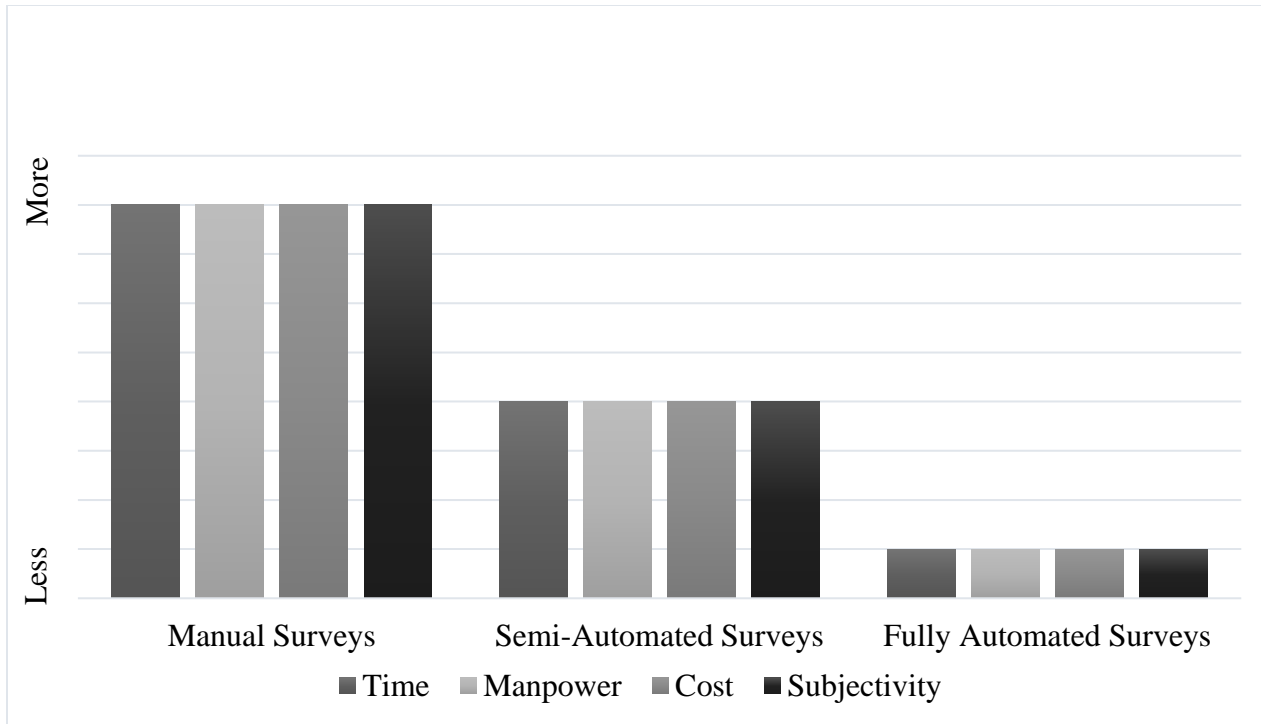


Figure 2.5: Comparison of the Traditional and Automated Pavement Assessment Methods Based on Time, Manpower, Cost, and Subjectivity of Evaluation

Specifically, UAVs have shown a potential in developing the automated pavement condition assessment methods with the maneuverability and ease of obtaining digital images for the pavements without being in contact with the actual pavements and utilizing them to develop the distress classification models. The evolution of UAVs for commercial applications and its use for various fields, as well as for pavement assessment are discussed in the subsequent sections.

### 2.5 Commercial Applications of Unmanned Aerial Vehicles (UAVs) in Different Fields

Formerly, UAVs were mainly used for military purposes such as surveillance and information retrieval for hostile territories. In the last two decades, UAVs are being adopted for commercial purposes such as data collection, disaster assessment and mitigation, construction, and transportation because of their efficiency and economy, effectiveness in enhancing situational awareness and ability to evaluate information (Floreano et al., 2015; Luppicini et al., 2016; Tanzi et al., 2016). With the impact made on the public and commercial spheres and the technological

advances in applications to enhance its functioning, UAVs are capable to improve and augment disaster management and recovery. They can be equipped with various attachments that could aid in the accumulation of precise information required to assess the situations after the natural disasters. The data gathered through them, in any crisis management scenario is critical to devise an appropriate emergency management response (Tanner, 2018).

Roads blocks and time constraints create difficulties for the response effort following a disaster. In many cases, damage to roads, buildings, and bridges prevent transportations networks from functioning efficiently. For the evacuation of victims, traditional airplanes and helicopters continue to provide the main pathway to safety, but for areas that cannot be reached by conventional aircraft, UAVs are proposed as an integral part of the emergency response phase. By providing much needed information to assess damages quickly and the delivery of critical supplies for affected people in non-accessible areas, they may become part of a relief distribution system as they can supply a large amount of demand in the least amount of time and can work without disrupting the ground transportation systems (Nedjati et al., 2016).

Specific to construction field, UAVs have proved to be an efficient tool for aerial photography, jobsite inspections, safety and security monitoring, construction land surveying and logistics management, and remote monitoring of jobsite progress (Ashour et al., 2016; Li et al., 2019; Tatum et al., 2017). Researchers have focused their efforts on adopting drones and developing techniques for surveying, assessing, and monitoring of civil infrastructures (Hallermann et al., 2013, 2014; Jordan et al., 2018; Liu et al., 2014; Sankarasrinivasan et al., 2015).

The key benefit of using UAV is that with its ability to capture a wide area and mobility to reach to restricted areas, it can aid efficiently in investigating civil structures (Kim et al., 2018). In addition, by attaching various cameras or combination of different cameras, the information

required for pavement defects, structural defects and other important data could be gathered. For example high resolution, zoomed in images of surface cracks, potholes, bleeding of asphalt, and so on (Ragnoli et al., 2018). Furthermore, it can also aid in visualizing the surface temperatures of pavements and the difference in temperatures along the pavement using multispectral imaging (Pan et al., 2018).

## **2.6 Automated Pavement Assessment Using Unmanned Aerial Vehicles (UAVs)**

Ground based traditional assessment methods for pavements are time consuming, expensive, and cumbersome. Employing drones for collection of pavement data is a resource saving and efficient means for roadway network analysis reducing field time and covering a broad area with more detailed information (DroneDeploy, 2018). A number of different studies have been conducted for the identification of pavement surface distresses using aerial images and image classification methods. Schnebele et al. (2015) provided a review the possible benefits of remote sensing techniques (e.g., UAV, LIDAR) in the rapid assessment of pavements by covering larger area in less time reducing the need for site visits and manual inspection.

Zhang (2008) presented a UAV based photogrammetric mapping system for the condition assessment of unpaved roads and used information by combining 2D and 3D image features through pattern recognition and image classification. The results reflected that UAV images can sufficiently extract many of the parameters needed for monitoring the condition of unpaved roads. In a later study, Zhang et al. (2012) developed a digital image-based system for the collection of data for rural roads for creating 3D models of the surface distress using image processing algorithms, and compared the extracted 3D information with the onsite measurements of the pavement distresses to test the performance of the digital image-based system. The 3D reconstruction of the onsite distresses allowed near accurate measurements up to 0.5 cm for the

characteristics of the distress on the computer application indicating promising results of the developed system.

Li et al. (2019) analyzed UAV LIDAR (Light Ranging and Detection) point cloud data using Random Forest Classification (RFC) to identify asphalt pavement defects. Through the UAV LIDAR point cloud data, the spectral and spatial information of the pavement distresses was extracted to develop the RFC model. A total of 48 features (e.g., elevation, intensity, roughness, curvature, geometric) were incorporated in the model and it was discovered that this information proved effective in the detection of the pavement defects. It was deduced that the UAV LIDAR data proved to be an efficient tool in the pavement condition assessment. The accuracy of the analysis from RFC method was evaluated against results from Support Vector Machine (SVM) and Maximum Likelihood (MLC) classifications and the results of RFC were found out to be more accurate. The overall accuracy for the distress identification proved substantial, validating the stability of the method to substantially evaluate pavement condition and implement maintenance.

Helali et al. (2008) performed a comparative analysis of pavement data before and after hurricane events indicating the damage to the pavement structure was evaluated through statistical techniques (T-test and ANOVA) for both Hot Mix Asphalt (HMA) and Portland Cement Concrete (PCC) pavements. The data before hurricane was extracted from the PMS which provided crucial information of the pavement condition pre-hurricane. The data after hurricane for the pavements under examination. The sectional level analysis involved evaluating the rate of deterioration by comparison with the predicted performance of each section to the actual performance and identifying the average rate of deterioration based on historical data. The results of the functional analysis showed that flooded pavements were significantly more damaged and more so the HMA pavements than PCC pavements.

Inzerillo et al. (2018) utilized UAV aerial images and images taken directly by operators with Structure Form Motion (SfM) (i.e., UAV-SfM and N-SfM respectively) to create 3D reconstruction models for the pavements to bring improvement in the automatic distress detection process and increasing the reliability of these methods. The resulting SFM models were compared with terrestrial laser scanned model to inspect the metric and visual accuracy. The collected data was imported to Photoscan, a computer application, to process and visualize the reconstructed models. It was deduced that the metric accuracy was greater for the N-SfM model, however, UAV-SfM enabled rapid identification of pavement distresses and the condition of road on a large-scale. Therefore, UAV-SfM models can prove to be useful for a preliminary survey of the roads whereas, N-SfM models can be created for detailed assessments.

Saad et al. (2019) analyzed two pavement distresses (i.e., potholes and ruts) for flexible pavement sections using images from a multicopter unmanned aerial vehicle (UAV) and processing the images using a photogrammetric software which is based on structure from motion (UAV images with Agisoft Photoscan software) which creates a 3D model and orthophoto product for the distresses. This system provides detailed and accurate measurements of road rut and pothole when compared with field measurements, and thus improves the efficiency of road condition monitoring. Khan et al. (2015) worked on acquiring non-contact, multispectral images using UAV systems for the preliminary investigation of bridges, assessing deck conditions (i.e., cracks, delamination) of common highway bridges. The results of the multispectral non-contact imaging system proved beneficial in revealing the deteriorated areas and locations on the bridge specimen and the actual bridge and have significant advantage in providing rapid assessment of bridge decks and other areas of interests. Ellenberg et al. (2014) evaluated the viability of UAV's remote sensing, aerial imaging capabilities in analyzing civil infrastructure deformations. The UAV

image-based evaluation was compared using both the data from TRITOP (an optical metrology system using a 16-megapixel digital single-lens reflex (DSLR)) and X-Box Kinect Device (which provides the red-green-blue (RGB) images with distance measurement) for the quantitative evaluation of the infrastructure. The objective was to develop computer vision photogrammetry techniques using UAVs images for evaluation of the deformed civil infrastructure, similar to visual inspection. The results indicated the ability of the developed technique effectively and accurately identified and evaluated the defects.

To fully understand the performance of the civil infrastructures especially pavement surfaces, various applications in computer visions such as machine and deep learning models have been developed for object detection and image recognition. There are several models including RFC, MLC, SVM, CNN which classify objects and images based on the features and images from the input data entered into these models. The next section discusses image classification approaches adopted for pavement condition assessment and distress classification.

## **2.7 Image Classification for Pavement Condition Assessment**

Image classification is used to analyze the information from digital images, where the process involves pre-processing images, object detection, feature extraction, and model training and validation. Various machine and deep learning algorithms have been developed and are used for performing image classification such as Support Vector Machine (SVM), Maximum Likelihood Classifier (MLC), Random Forest Classifier (RFC), Deep Neural Networks (DNNs) and Convolutional Neural Networks (CNNs). Several studies to identify defects for pavements on sectional level have been performed using UAV and image classification. The image classification methods, which have deep learning as their basis, have proven to be successful for computer vision tasks such as image recognition because of their ability to extract and learn appropriate features

while creating a distinction between them (Deng, 2014; Guo et al., 2016). Table 2.1 provides review of the most relevant studies on pavement distress classification found in the literature.

Table 2.1: Relevant Studies Reviewed in the Literature on Image Classification

Study	Data Collection	Classification Model	Image Pre-processing	Defect/ Distress Detected	Accuracy
Zakeri et al. (2016)	Quadcopter Unmanned Aerial Vehicle (QUAV) with GoPro Camera	Polar Support Vector Machine (PSVM)	Image Enhancement and Thresholding	Cracking (Flexible Pavements)	93-96%
Ersoz et al. (2017)	Unmanned Aerial Vehicles (UAVs) “DJI Inspire 1 Quadcopter”	Support Vector Machine (SVM)	Image Pre-processing (RGB to Grayscale, Segmentation, Thresholding, Binarization using median filtering and morphological operations)	Crack or No Crack (Rigid Pavements)	97%
Gopalakrishnan et al. (2017)	Data was used from the Federal Highway Administration’s (FHWA’s) Long-Term Pavement Performance (LTPP) program	Deep Convolutional Neural Network (DCNN) “VGG-16 Model” (Pre-trained Network)	Pre-processed raw images to eliminate the outer edges of the image (views of the shoulder and/or centerline)	Crack or No Crack (Both HMA and PCC Pavements)	90%
Gopalakrishnan et al. (2018)	Hexacopter UAV with high-definition camera (Canon EOS 5D Mark IV DSLR)	Deep Convolutional Neural Network (DCNN) “VGG-16 Model” (Pre-trained Network)	None	Crack or No Crack (Infrastructure)	90%
Li et al. (2019)	Raw images of Concrete Surfaces	Convolutional Neural Network “AlexNet” (Pre-trained Network)	None	Crack or No Crack (Concrete Structures)	99.06%
Ibragimov et al. (2020)	High-resolution Camera mounted on a Vehicle	Faster Region Based Convolutional Network (R-CNN)	Annotated Bounding Boxes	Cracking (Linear and Area) and Patching (Flexible Pavements)	38.1%, 77.1% and 84.6%

Zakeri et al. (2016) established a procedure for the automated detection and identification of cracks in flexible pavement, named Polar Support Vector Machine (PSVM), based on Support

Vector Machine (SVM) classifier. The study focused in designing a multi-stage system (MSS) for quadcopter unmanned aerial vehicle (QUAV) image analysis consisting of image processing, threshold selection, and classification stages for automatic inspection of pavement cracking. The research findings indicated reliability of the model prediction ranging between 93% - 96% in identifying the cracks when compared to the other classifiers such as SVM and NN and showed potential for future practice in pavement assessment.

Ersoz et al. (2017) used unmanned aerial vehicle images and image classification algorithm, Support Vector Machine (SVM), for the identification of cracks in rigid pavement sections. The DJI Inspire 1 Quadcopter (UAV) was used to capture aerial images of the cracked and non-cracked regions of rigid pavements around the Middle East Technical University (METU) campus. These RGB images were then processed and converted into grayscale images and a threshold for segmentation was applied individually to all the images. These images were then converted into binary images using median filtering and morphological operations for training the SVM model. This method provided successful results in differentiating the cracked and non-cracked regions and with an accuracy of 97%. However, the model lacks sensitivity as it has difficulty in extracting crack from the images that contain both crack and non-cracked regions or shadows, which can be improved by using a larger dataset.

Gopalakrishnan et al. (2017) performed a deep convolutional neural network (DCNN) classification to identify cracked and non-cracked pavement regions based on transfer learning approach using the pretrained network VGG-16 DNN. The results were also compared with other classifiers which include Support Vector Machine (SVM), Random Forest (RF), Logistic Regression (LR), and Extremely Randomized Trees (ERT). It was discovered that the DNN yielded best results with an accuracy of 90% followed by SVM with an accuracy of 87%. On

another study, Gopalakrishnan et al. (2018) proposed using a pre-trained deep neural network (DNN) “VGG-16” model for the automatic crack damage detection in UAV images of civil infrastructure. The trained DNN enables damage detection through automated or semi-automated techniques and the rapid assessment yields 90% accuracy in detecting cracks in realistic situations without any augmentation and preprocessing.

Li et al. (2019) established an image-based crack detection approach using a pre-trained deep convolutional network “AlexNet” and modifying it to identify cracks on concrete structures. The methodology involved taking a large number of raw images of concrete surfaces and creating a database for training the CNN model to perform the classification for images with and without cracks. The resulting model yielded a validation accuracy of 99.06% showing promising results in concrete crack detection and the developed model was integrated into a smartphone application “Crack Detector” which was based on the framework of Core ML, for the ease and accessibility in crack detection process.

Ibragimov et al. (2020) proposed a faster region based convolutional network (R-CNN) approach to detect pavement distresses focused on identifying cracking (longitudinal, transverse, and alligator) and patching in pavements. The study involved gathering pavement images using a high-resolution camera mounted on a vehicle and using annotated bounding boxes to label the distress categorized as linear crack (longitudinal and transverse cracks), area crack (alligator cracks), and patching. The image database was created by splitting the images and labelling the distresses using bounding boxes for training the classifier. The results indicated an average precision of 38.1%, 77.1%, and 86.4% for linear cracks, area cracks, and patching, respectively.

Although the literature reviewed indicate that automation in the pavement condition assessment brought by digital image processing and image classification models have potentially

beneficial results in making the evaluation rapid, safe, and objective. However, most of these studies identify whether there is a specific distress (cracking), or if there is a distress or not (crack or no crack) and only one study classifies three distresses. In addition, some of the studies also rely on image pre-processing such as image enhancement, image thresholding, and annotated bounding boxes to extract relevant information for the model. Furthermore, the studies also utilize different equipment and data collection techniques such as camera mounted on a vehicle, FHWA's pavement database, digital cameras. This research aims develop a rapid method for pavement condition assessment through classification of two types of distresses (i.e., alligator and longitudinal cracks) based on a single equipment (UAV) for the faster and efficient acquisition of aerial imagery and limiting physical presence on-site and increasing safety. The gathered aerial images are not pre-processed and used in their raw form for the image classification model (CNN), so the time for image processing is also reduced. The study uses a single platform (MATLAB) for the development of the CNN model and no other computer applications are used. With this said, this study provides a theoretical base for further improvements in the automated pavement condition assessment methods. The methodology used for the research is explained in the next chapter.

## **CHAPTER 3: METHODOLOGY**

### **3.1 Introduction**

This chapter focuses on the methodology used in the development of pavement distress classification model, which includes collection of pavement condition data using drones, as well as CNN model development. This chapter begins with definitions of basic terms that are used throughout the remainder of the thesis. The chapter then outlines the rationale and methodology behind the data collection and the development of the classification model.

### **3.2 Definitions**

In this study, several terms are used to describe pavement conditions and types, pavement cracks, and pavement condition assessment (e.g., pavement distress, longitudinal cracking, alligator cracking, pavement rapid condition assessment). Other important terms in reference to the image classification and CNN models are also used. Defining these terms is vitally important to facilitate understanding the developed model. This chapter explains the following definitions in the context of this study:

- **Pavement Distress:** Pavement distresses are defects in the pavement structure resulting from the combination of effects from traffic loading and environmental conditions, leading to a poor and undesirable pavement performance and impending pavement failure.
- **Flexible Pavement:** A pavement in which the surface layer is constructed with asphalt or bituminous material.
- **Longitudinal Cracking:** Longitudinal cracks are surface defects which occur in the direction of the wheel path parallel to the center line of the road. Continual deterioration of the roads with longitudinal cracks eventually lead to other parallel, transverse, and alligator cracks. Longitudinal cracking indicates beginning of possible fatigue cracking and structure failure and results in moisture infiltration and pavement roughness.

- Alligator Cracking: Alligator cracking, also known as fatigue cracking, occurs on the surface of flexible pavements. It is in the form of interconnected cracks shaped as small irregular pieces of pavement, resulting from fatigue failure. As a consequence, there is moisture infiltration and increased roughness of pavements.
- Image Classification: It refers to the extraction of information from the input images and classifying them into a set of predefined categories.
- Rapid Pavement Condition Assessment: Over the years, there have been improvements in the pavement surveys and assessment methods, with several semi-automated and automated methods significantly reducing time and labor requirements. The method presented in this research is rapid in that it proposes the use of aerial images through UAVs which reduces the manpower, time, and equipment required for field surveys for data collection. The data collected can then be passed through the image classification model for the identification of distresses which can be performed in the field or offsite.
- Convolution: Mathematical operation in CNN in which a filter is applied to an input and the resulting product is an activation (i.e., product of two matrices to produce a third function “activation”).
- Kernel or Convolution Filter: Matrix of random numbers with smaller height and width, but the same depth as of the input image used in CNN model.
- Stride: It is the number of pixels that the filter moves over the input matrix from one position to the other (e.g., if the stride = 1 then the filter slides over by one pixel value) in CNN model.
- Weights: A measure of how much influence the input data will have on the output in between the network layers.

- Biases: A constant additional set of weights which require no input (i.e., they do not have any incoming connections) but act as an input to the next layers with their own weights.

### 3.3 Rapid Pavement Condition Assessment Methodology

The overall goal of the proposed rapid pavement condition assessment is to improve pavement condition assessment in general and the classification of pavement distress after hurricane events in particular. (Figure 3.1) illustrates the major steps undertaken for the research methodology:

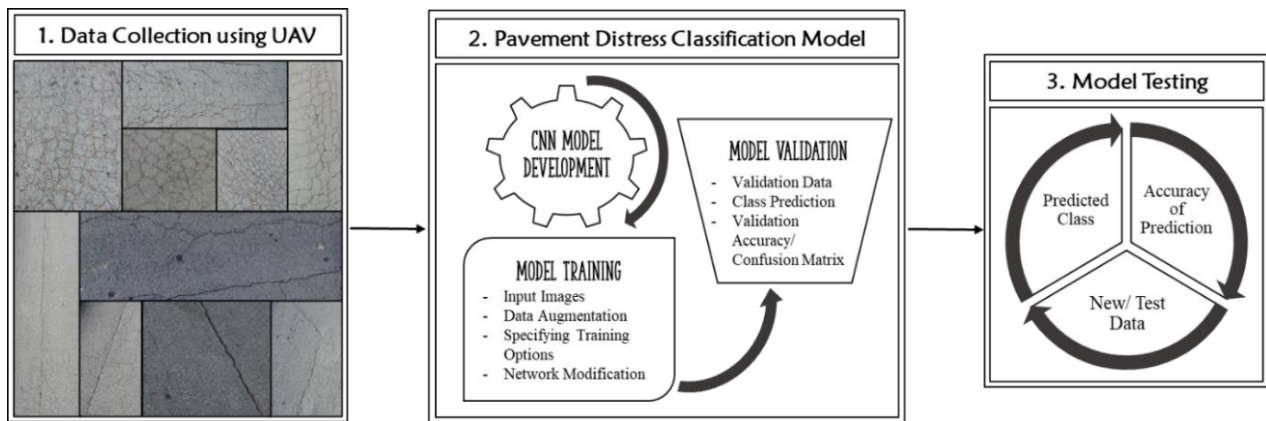


Figure 3.1: Research Methodology Roadmap

1. Data Collection using UAV: High resolution aerial images for pavement distress were collected using Unmanned Aerial Vehicles (UAVs). The images were collected for damaged pavement on multiple locations on East Carolina University (ECU) campus.
2. Pavement Distress Classification Model: A deep learning model based on Conventional Neural Network (CNN) was established using the high-resolution aerial images to classify two types of pavement distress (i.e., alligator cracks and longitudinal cracks).
3. Model Testing: To test the model’s performance in practice, a new set of images were introduced to gauge the prediction accuracy of the model.

The following sections illustrate the data collection using UAVs, description of the CNN network architecture, image classification through CNN, and the modification of the pretrained network for the classification of pavement distresses using a deep learning model, “AlexNet” a pre-trained network.

### 3.3.1 Data Collection using UAV

This section explains the process of rapidly and safely collecting high-resolution aerial images of pavement distresses using the advanced technology Unmanned Aerial Vehicles (UAVs). Streets with flexible pavements around East Carolina University (ECU) campus were selected with the two types of surface distress considered for this research (i.e., alligator cracks and longitudinal cracks). Figure 3.2 shows a map for the streets surveyed on ECU campus.

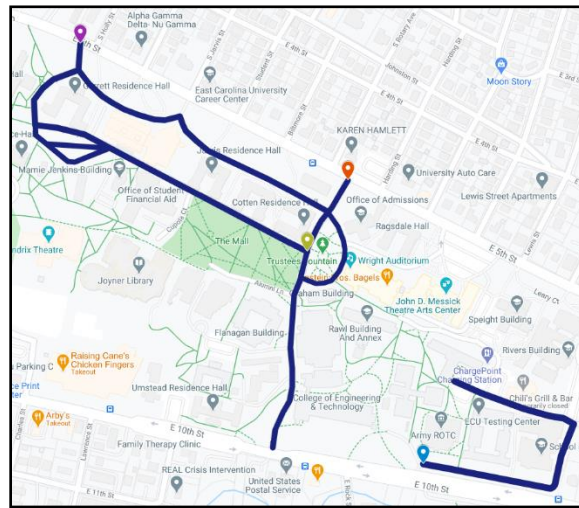


Figure 3.2: Locations of Surveyed Streets with Pavement Distresses on ECU Campus

The aerial images were captured by flying the DJI Mavic Mini UAV at a height of 10-15 ft above the pavement surface. The UAV weighs approximately 0.5 lbs. and is 0.5 ft x 0.5 ft x 0.2 ft in size (Figure 3.3). It has a built-in camera with 1/2.3-inch CMOS sensor and effective pixels equal to 12 MP. The UAV flight was manually operated to maintain safety and avoid any collisions or accidents and the streets were surveyed in segments of single flights in one direction. The

camera attached recorded the video for the whole span of the streets and the images were then extracted from the collected videos. The aerial imagery obtained was cropped to represent the distresses in post-processing to get the desired results. The collected aerial images were manually labeled and classified into the two categories before inputting them into the model.



Figure 3.3: DJI Mavic Mini Used for Data Collection

### 3.3.2 Pavement Distress Classification Model

This section illustrates the development of the pavement distress classification using high resolution aerial images collected from UAVs. To achieve this, a deep learning model, “AlexNet” a pre-trained network based on Convolutional Neural Networks (CNNs) is adopted. The following sections provide a description of the CNN network architecture, image classification through CNN, and the modification of the pretrained network for the classification of pavement distresses.

To assess pavement condition, CNN, which stems from the field of deep learning and comprises of a deep network architecture with several hidden layers (Xie et al., 2017) is used as the image classification approach. CNN classifies images by perceiving information from the raw input data and then learning from the features of these data. CNNs are being widely used for various classification problems including structural damage detection, road damage detection, pavement crack analysis, and distress detection (Abdeljaber et al., 2018; Nie et al., 2018; Wang et

al., 2018; Wang et al., 2017). The CNNs have two main components: 1) feature extraction and 2) classification (Figure 3.4) and the CNN network architecture consists of visualized layers (i.e., convolutional layers, max pooling layers, fully connected, and softmax layers) and other functional layers (i.e., rectified linear unit (ReLU) layers, local response normalization (LRN) layers, and dropout layers).

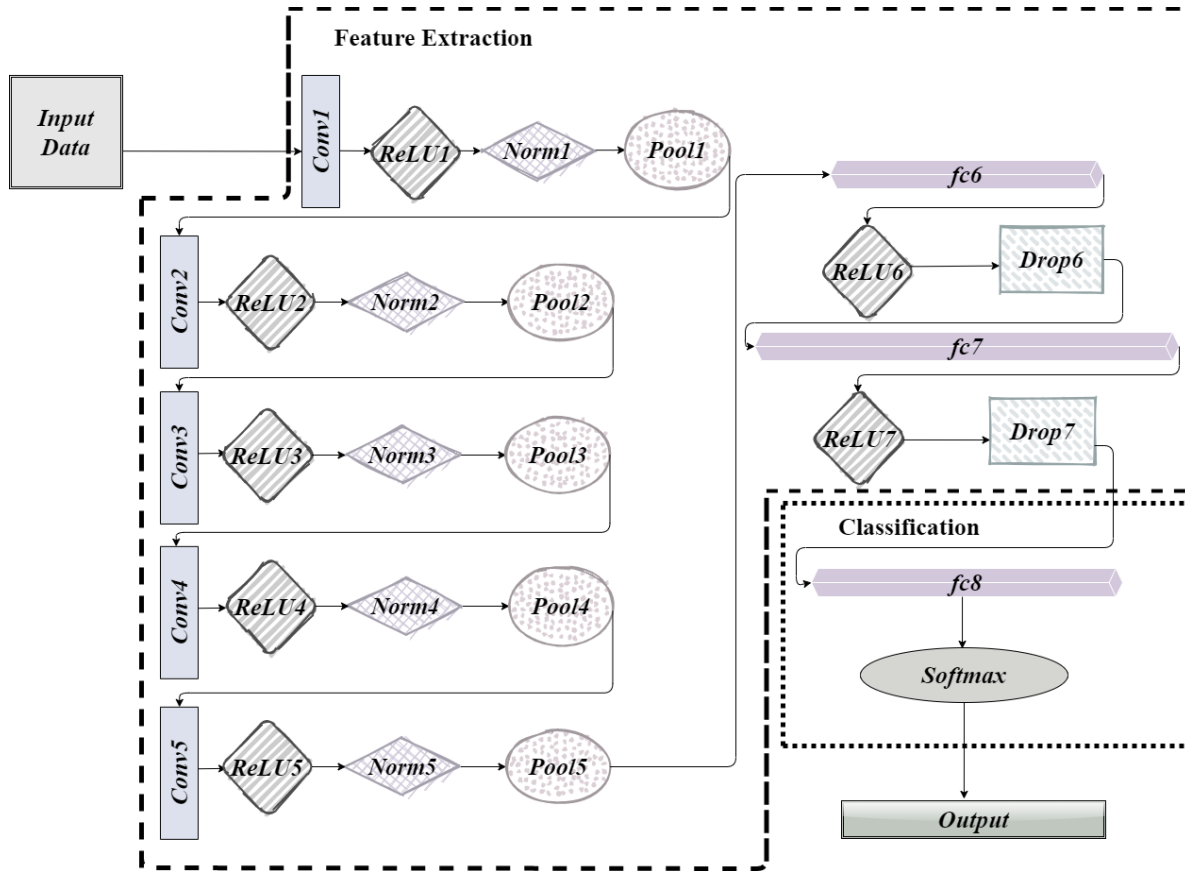


Figure 3.4: Architecture of Conventional Neural Network (CNN)

### 3.3.2.1 Feature Extraction

Two main operations (i.e., convolutions and pooling operations) and three secondary operations (i.e., ReLU activation, normalization and dropout operations) take place in the feature extraction part. Main operations take place in the convolutional, and pooling layers, while the secondary operations take place in the rectified linear unit (ReLU), local response normalization

(LRN), dropout layers. The rationale behind the main operations is detecting features of the input images, while the rationale behind the secondary operations is enhancing the network performance.

1. Convolution operation: It takes place in the convolution layer and it uses a convolution filter or kernel to extract features from the input images and generates a “feature map”. Convolution operation is applied to the pixel matrix of the input images using random filters, where each filter extracts certain features from the input image creating a set of convolved features (i.e., feature map) to be used as inputs for the next layer in the network. (Figure 3.5) shows the convolution operation with a pixel matrix of a 5x5 input image and 3x3 random convolution filter with a stride of 1. The filter slides over the of the input image pixels, shifting its position one pixel at a time, and perform a multiplication with the input image. The result of each multiplication between 3x3 pixel matrix of the input image and filter is then summed and added to create the feature map.

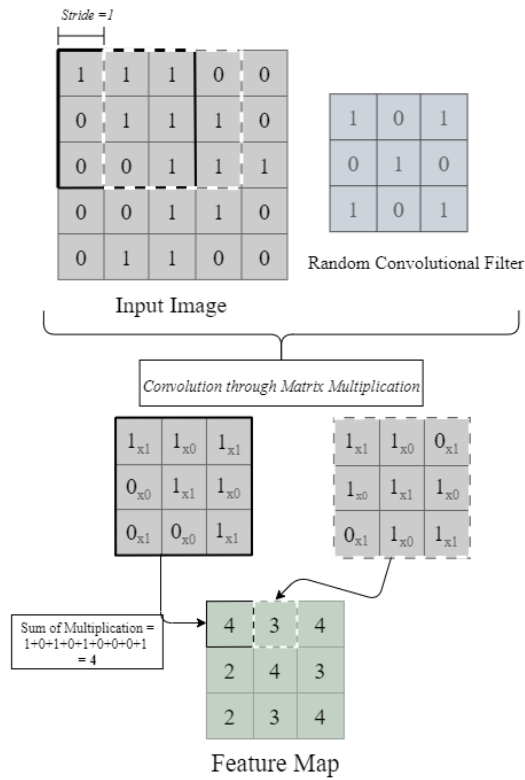


Figure 3.5: Convolution Operation of Conventional Neural Network (CNN)

2. Pooling Operation: It takes place in the pooling layer and it reduces the number of parameters and computation in the network by reducing the spatial dimensions of the input feature map and by taking the largest features from the rectified feature map (i.e., maximum pool value in each 2 x 2 matrix) (Figure 3.6). This operation shortens the training time and controls overfitting, consequently increasing the model's performance (Li et al., 2019)

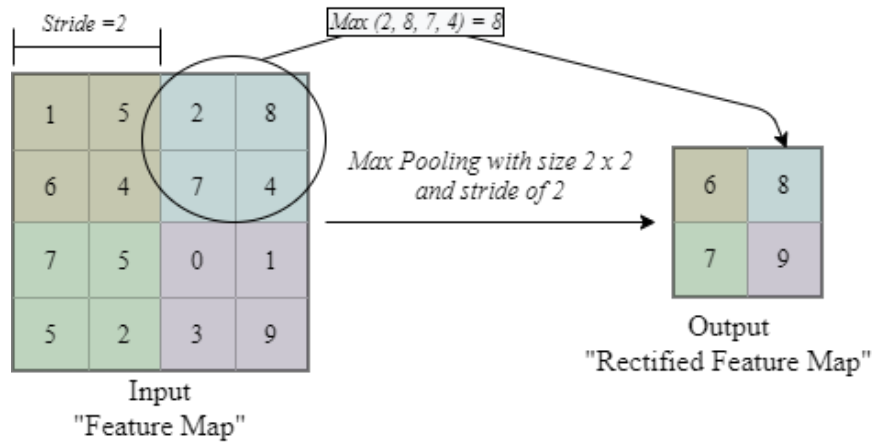


Figure 3.6: Pooling Operation of Conventional Neural Network (CNN)

3. **Activation Operation:** It takes place in the Rectified Linear Unit (ReLU) layer and it accounts for the non-linearities in the network. The operation is applied on the feature maps to convert all the negative pixel values to 'zero' and activates features with positive input values for learning, consequently, allowing faster computations for gradient descent training. The operation is performed using the following function " $f(x) = \max(0, x)$ " (Nair et al., 2010) where  $x$  is positive pixel value.
4. **Normalization Operation:** It takes place in the Local Response Normalization (LRN) layer and is applied on the unbounded ReLU features (i.e., features not bounded by a range of certain outcomes or values) to avoid saturation of the input features. The operation is applied by locating the high frequency features of ReLU (i.e., having higher numerical value) with relatively larger activations and making them more sensitive than their lesser activated counterparts, in order to normalize them, so that the network is unbiased to these high frequency features.
5. **Dropout Operation:** It takes place in the dropout layer and it accounts for overfitting. In CNN overfitting occurs either with a large number of training parameters or when the

network is trained on a smaller dataset. To eliminate overfitting, hidden features with a probability of 0.5 are randomly dropped off making them unaffected by the presence of other hidden features (Hinton et al., 2012; Srivastava et al., 2014).

### 3.3.2.2 Classification

One main operation (i.e., classification) takes place in the fully connected and Softmax layers, which serve as the classifier. The key purpose of the classification operation is combining the extracted features from the convolutional and pooling layers and then assigning probabilities to the categories of these features. For features with two categories, probabilities are calculated using logistic regression, while for features with more than two categories, probabilities are calculated using multinomial logistic regression. (Figure 3.7) illustrates the classification part of the CNN. For the two categories of pavement distress, the probabilities are calculated as:

$$P(w_j | n, \theta) = \frac{e^{\theta_j^T n}}{\sum_k e^{\theta_k^T n}}$$

where, ' $P(w_j | n, \theta)$ ' is the probability associated with the class ' $j$ ' during the observation ' $n$ ' and ' $\theta$ ' are the model parameters.

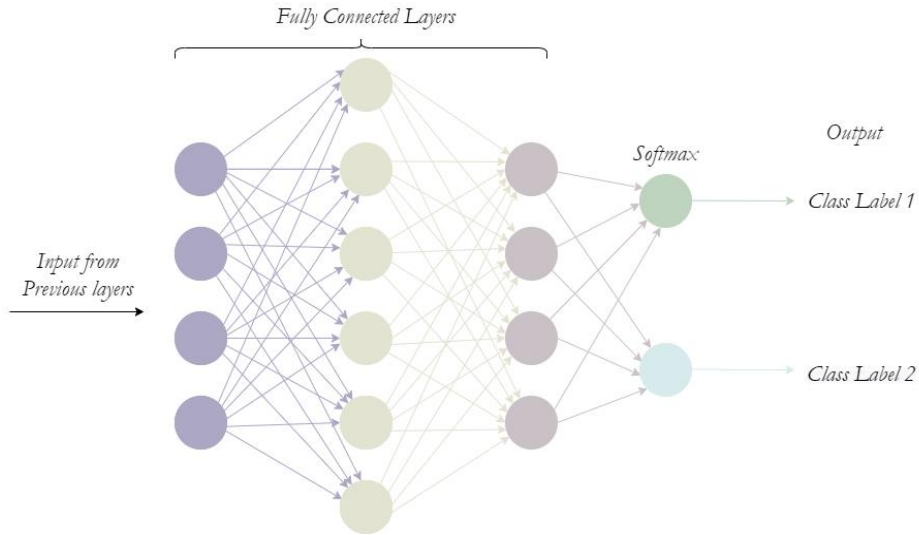


Figure 3.7: Layers Involved in the Classification Part of Conventional Neural Network (CNN)

### 3.3.2.3 AlexNet Conventional Neural Network (CNN)

For greater prediction accuracy, large datasets are required to train the CNN model, which is not always convenient to acquire. Therefore, transfer learning approach using AlexNet, a pre-trained CNNs, is adopted. In this approach, a pretrained model is modified to transfer the pre-designed learnable parameters (i.e., weights and biases), to a new classification using a new and smaller dataset (Gopalakrishnan et al., 2017). In this study, a pre-trained CNN model, “AlexNet” is modified in MATLAB for the pavement distress classification. AlexNet is a network trained on more than a million images from ImageNet database and has learned rich feature representations for a wide range of images to classify 1000 object categories (Krizhevsky et al., 2012). All the feature layers are considered for the modified network except the last two layers of the network (i.e., final fully connected and the softmax layers) which are initially configured to classify 1000 objects. The transformation enables the network to be reconfigured to identify two classes of the pavement distresses. The properties of these layers are replaced so that they only classify the input into two categories instead of 1000 as indicated in the non-modified network. The alterations made are as follows: the fully connected layer “fc8” is renamed as “fc” with new weights and bias learn

rate factor (i.e., 20 for both), and the softmax layer is customized to enable detection of the new categories; therefore, the image classification is modified to two categories.

### 3.3.2.4 Model Training

The CNN model was established in MATLAB R2020a in a Windows system configured with a GPU. The system specifications are as follows; Processor: Intel® Core™ i7-9750H @ 2.60GHz 2.59GHz, RAM: 16GB, and GPU: NVIDIA® GeoForce RTX™ 8GB GDDR6 with Max-Q Design. The dataset consisted of 100 images and the categories of pavement defects were predefined as alligator and longitudinal cracks. The original dataset was divided randomly into two subsets, training, and validation. The training subset comprised of 70% of the original images and was used to train the CNN model and the validation subset comprised of the remaining 30 % of the original dataset and was used for model validation. The categories and number of images in each category for training and validation sets are shown in (Table 3.1).

Table 3.1: Pavement Distress Categories and Frequency of Collected Data for Training and Validation

Categories	Training Set	Validation Set	Total
Alligator Cracks	35	15	50
Longitudinal Cracks	35	15	50
Total	70	30	100

The high-resolution aerial images collected from UAV were inputted for training the CNN model. These datasets were augmented to fit the network requirements, such as resizing images to 227x227 size for the input layer, and it also prevents overfitting the model. The model trains on the input images from the training dataset using a stochastic descent gradient (SGD) algorithm with momentum which updates the network parameter after each input during the training process. The model training is initialized with random weights and bias which leads to deviations in the

actual and predicted classes, yielding a poor performance of the model when the training begins. The SGD with momentum algorithm enables a reduction in this divergence by updating weights and optimizing the loss function (Li et al., 2019). The algorithm accelerates the convergence speed of training by increasing the momentum for vectors whose gradients head in the same direction and decreasing the updates for parameters whose gradients switch directions (Ruder, 2016). The training options set for the CNN models are as follows:

The number of images used per update is a subset of the training dataset and is referred to as the “mini-batch size” which is specified as ‘35’. Every parameter update that takes place out of the specified batch size is called an “iteration” and a full pass or complete update of the entire dataset is called an “epoch”. The maximum number of epochs was set to ‘6’. The initial learn rate is set to ‘0.0001’. The training data is shuffled ‘once’ before training. Selecting a feature layer for the CNN model is a design consideration, for this model, the feature layer is specified as ‘drop 7’ which extracts the distress features for the CNN model for this classification task.

The data passes through the convolutional layer, where the image features are extracted through the convolution process and a “feature map” is generated. The feature map is then fed into the ReLU layer which replaces the negative pixel values with zero and it accounts for non-linearities in the network yielding a “rectified feature map”. The rectified feature map is then normalized in the LRN layer to avoid saturation of the input features, after which the pooling operation occurs that enables the network to take the largest element from the rectified feature map forward, consequently reducing the number of learning parameters. A dropout function is also applied 0.5 probability factor to the features with from ReLU layer to eliminate overfitting. The fully connected layer combines the extracted features from the convolutional and pooling layers to classify an image into a particular class with the help of a softmax function. The softmax

function assigns probability values for the multiple categories of classification indicating that a certain feature is representative of a certain category and the operation is administered just before the output layer, therefore, the softmax layer contains an equivalent number of neurons as the number of categories (i.e., one output for each class).

### 3.3.2.5 Model Validation

After the CNN model is trained in section 3.2.3, the predictive performance of the CNN model was validated using cross validation. Cross validation is a technique to estimate the accuracy at which the model will perform in practice, illustrating the model's ability to predict new or unseen data. The validation subset comprising 30% of the original dataset is used to perform the cross validation. Model performance was assessed by finding the cross-classification rate (CRR), which indicates the percentage of pavement distress where predicted distress class corresponds to the observed distress. The percentage of the correctly classified distress is calculated as:

$$CCR = \frac{\sum_{d=1}^D F_{dd}}{\sum_{d=1}^D \sum_{c=1}^C F_{cd}}$$

### 3.3.3 Model Testing

Model testing was carried out by introducing a new set of images or test images to the model and determining the performance of the model in practice. The test data consisted of a total of 10 images from both the trained categories (alligator and longitudinal cracks), five in each category, and were uploaded to the model for individually to determine the model performance and the accuracy of prediction. The model performance was estimated based on the cross-classification technique, similar to model validation, and finding the cross-classification rate based on the number of images used in the test set and their predicted class labels from the model.

## **CHAPTER 4: RESULTS**

The overall goal of this study was to better understand the performance of pavements and bring an improvement in the pavement inspection methods by developing a procedure that enables rapid pavement condition assessment. To accomplish this goal, three main objectives were defined. The first objective, which involved review of existing pavement condition assessment practices, revealed a need for rapid and automated approaches. As discussed in Section 2.6 several existing practices that were reviewed had focused on 1) using traditional data collection approaches and not advanced approaches (i.e., UAV) to collect pavement data and 2) identifying whether or not there is a specific distress without specifying the type of distress. Therefore, the remaining objectives were directed towards meeting these needs: 1) collecting high resolution aerial images for pavement structures using Unmanned Aerial Vehicle (UAV) and 2) classify two categories of pavement distress through the development of deep learning image classification model. Methodology behind these two objectives is presented in Chapter 3, and this chapter presents results of the classification model.

### **4.1 Pavement Distress Classification Model**

The basic process of image classification through Convolutional Neural Networks (CNNs) is presented in Chapter 3 and it involves the following steps: 1) loading the input image data into the model which then passes through the layers of the network, 2) learning the features from the images and creating feature maps, and 3) classifying the pavement distresses. The pavement distress classification process is illustrated in (Figure 4.1).

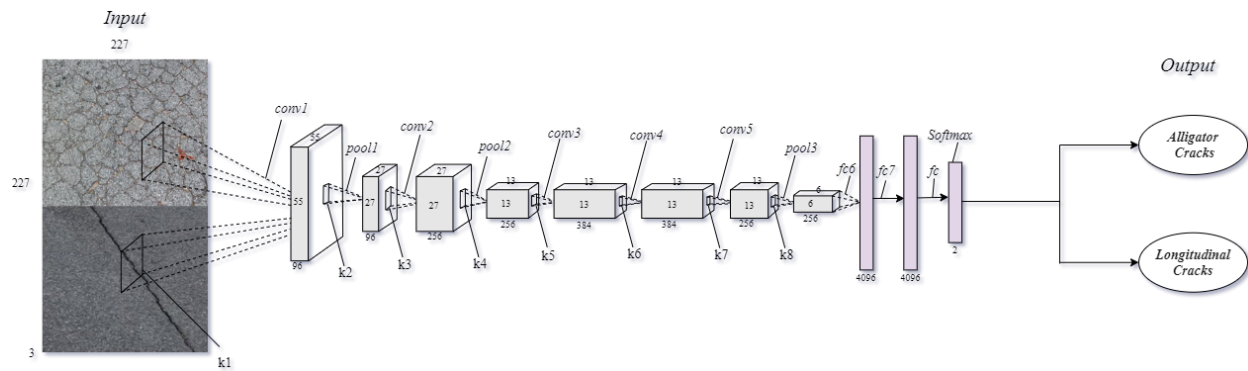


Figure 4.1: Pavement Distress (Alligator and Longitudinal Cracks) Classification Process using CNN

The CNN model was trained using a training set that counts for 70% of the original dataset.

A randomly generated array of images for model training is shown in (Figure 4.2).

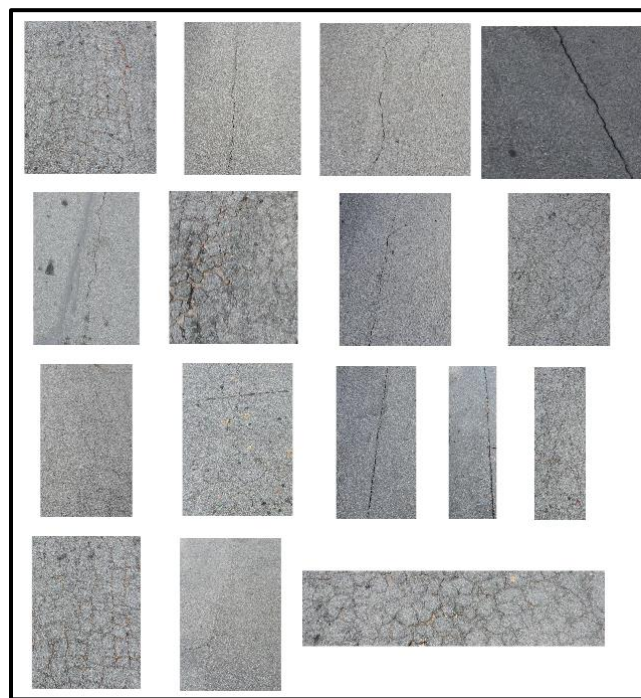


Figure 4.2: Array of Random Images of Pavement Distress used for Model Training

Results of model training is illustrated in (Figure 4.3). The accuracy and loss during training is indicated with the blue and orange lines in the graph, respectively. The training accuracy gradually increases (i.e., from approximately 58 % to 97%) as the algorithm passes through the dataset with each epoch updating the parameters and learned features. Simultaneously, the loss

during the training is reduced over the epochs increases (i.e., from approximately 1.1 to 0.18). The dotted line represents the accuracy and loss based on the validation data set for which a similar trend is observed (i.e., an increase in accuracy and decrease in loss) over the subsequent epochs.

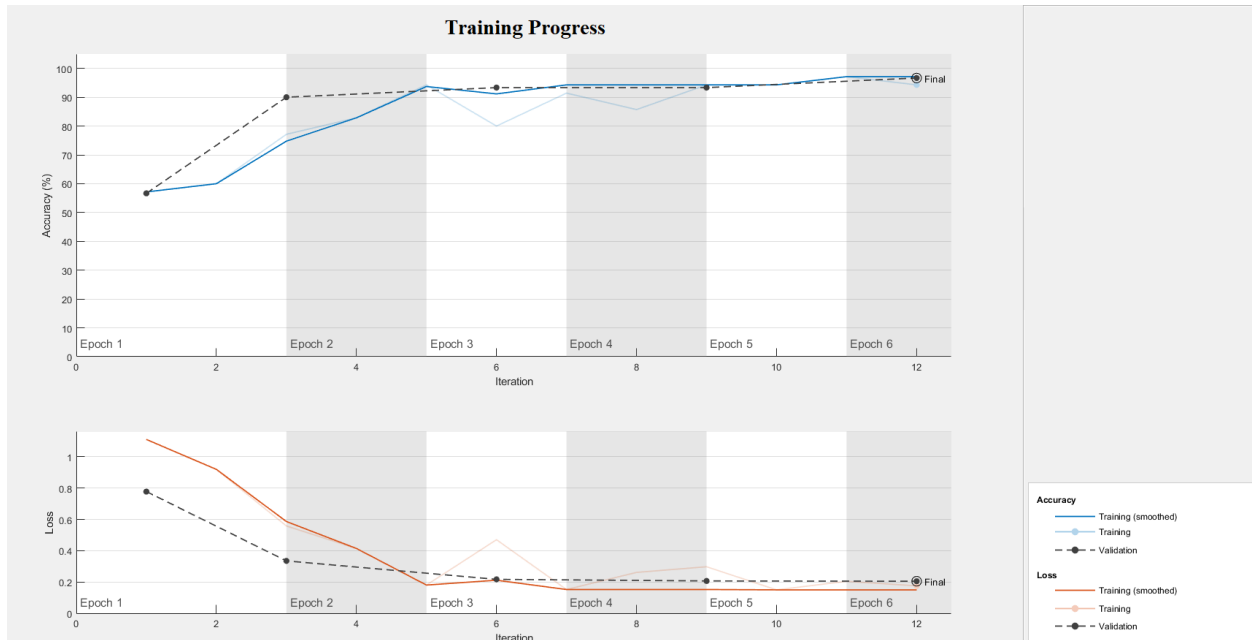


Figure 4.3: Training Process Indicating Accuracy and Loss during Model Training

## 4.2 Model Validation

The predictive performance of the CNN model was validated using a validation set that counts for 30% of the original dataset. The validation accuracy was represented every 3 iterations during the training in (Figure 4.3). The overall model accuracy is represented by the confusion matrix (Figure 4.4) and was found to be 96.7%, misclassifying only one image in for a single class during model validation which indicated a satisfactory model performance. The output class refers to the prediction from the model, whereas the target class refers to the actual label of the input image. The diagonal from left to right represents the correctly classified quantity (the number on top) and the correctly classified percentage (the percentage on bottom) of the corresponding categories.

		Target Class	
		Alligator Cracks	Longitudinal Cracks
Output Class	Alligator Cracks	<b>14</b> 46.7%	<b>0</b> 0.0%
	Longitudinal Cracks	<b>1</b> 3.3%	<b>15</b> 50%
		Total Accuracy <b>96.7%</b>	

**Confusion Matrix**

Figure 4.4: Model Validation Confusion Matrix

### 4.3 Model Testing

After model training and validation, the model was tested with a new set of images which were uploaded into the model independently to evaluate the accuracy of prediction in case a new dataset is collected. A total of 10 images were tested (5 for each category) and (Figure 4.5) illustrates the result of the images that were uploaded separately and represent the inputted image and the predicted class label. A misclassification similar to model validation was encountered during model testing, when the input image predominantly consisted of ‘alligator cracks’ but was incorrectly classified as ‘longitudinal cracks’ as represented in (Figure 4.6). This reiterated the inaccuracy of the model to incorrectly predict at least one image for a category in actual practice.

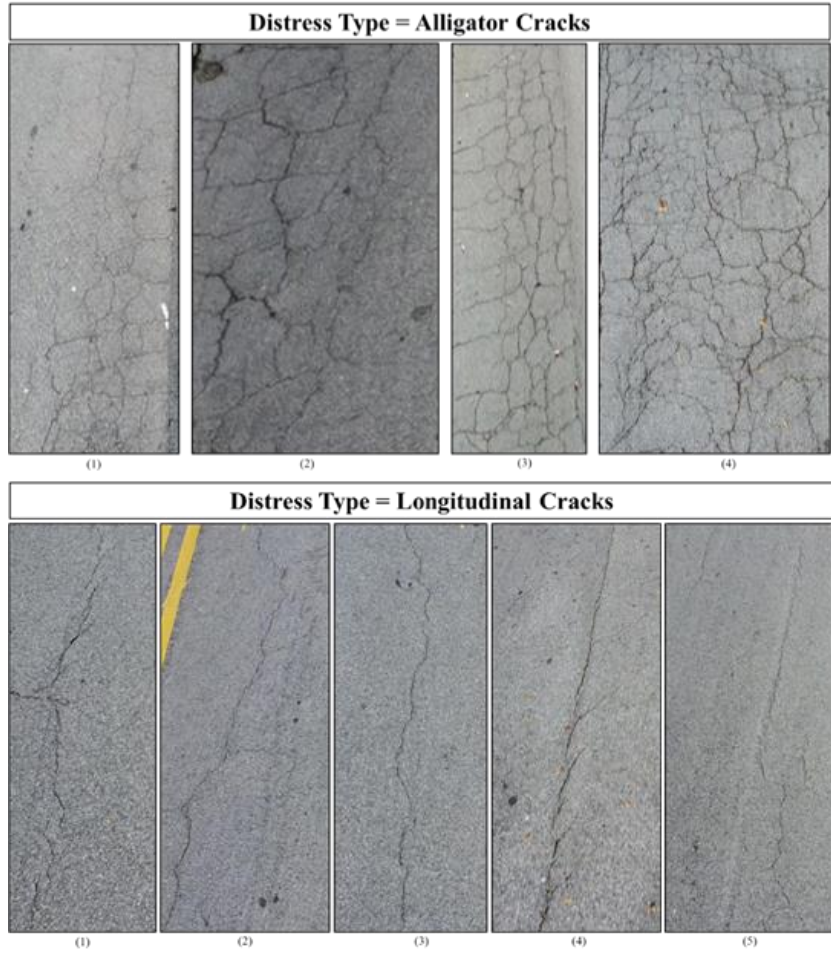


Figure 4.5: Model Testing (Correctly Classified Images from the Model)

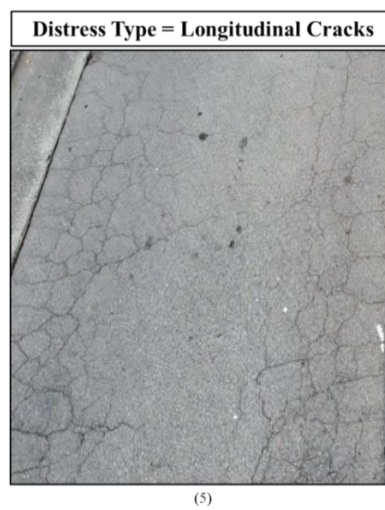


Figure 4.6: Model Testing (Misclassified Image from the Model)

A confusion matrix is given in (Figure 4.7) indicating the prediction accuracy during model testing. The overall testing accuracy is represented by the confusion matrix (Figure 4.7) and was found to be 90.0% based on the number of input images. Similarly, the output class refers to the prediction from the model, whereas the target class refers to the actual label of the input image. The diagonal from left to right represents the correctly classified quantity (the number on top) and the correctly classified percentage (the percentage on bottom) of the corresponding categories.

		Target Class	
		Alligator Cracks	Longitudinal Cracks
Output Class	Alligator Cracks	<b>4</b> 40.0%	<b>0</b> 0.0%
	Longitudinal Cracks	<b>1</b> 10.0%	<b>5</b> 50%
		<b>Total Accuracy 90.0%</b>	

**Confusion Matrix (Testing)**

Figure 4.7: Model Testing Confusion Matrix

## **CHAPTER 5: CONCLUSIONS AND RECOMMENDATIONS**

### **5.1 Conclusions**

This study has resulted in the development of a rapid condition assessment model for flexible pavements. Specific contributions include the use of advanced technology (Unmanned Aerial Vehicle) to collect aerial imagery for flexible pavement distresses and development of a deep learning classification model (Convolutional Neural Network) for the classification of the two pavement distresses (alligator and longitudinal cracks) in MATLAB.

The specific conclusions of this study are:

- The use of UAV has proven to be an effective, safe, and rapid approach for data collection, especially after natural hazard events, when access to the affected area is restricted.
- Based on the overall accuracy, the developed CNN classification model has proven to be a successful approach for the automated pavement distress classification.
- The model performance tested on new dataset has shown acceptable results in accurately classifying the two categories of pavement distress.
- The analysis of aerial images using computer vision resulted in the reduction in of human effort and time spent in the field for assessing pavement condition.
- The finding from this research will aid transportation engineers in rapidly assessing the damages to pavements and devise a restoration or repair plan for pavements in a quick, effective, and economic manner.
- Application of the developed model will provide a platform to minimize the damage to the pavements, which is sometimes caused by traditional approaches for pavement assessment and make the examination process efficient and rapid.

- Refinement of the developed model will save time and cost, facilitate quick decisions on rehabilitation and recovery of the pavements, allow emergency responders to locate the safest route to take to reach the disaster struck area, after hurricane events.

## **5.2 Recommendations and Future Research**

The major contribution of this research lies in the methodology that has been developed to rapidly assess flexible pavement distresses. Overall, the intent of the methodology is to lay out a research roadmap to develop classification models for other pavement types and distresses either at a small scale (road level scale) or a larger scale (road network scale). This roadmap, however, still has room for further refinement to enhance the data collection and the developed model.

A CNN model may be developed from scratch instead of using a transferred learning approach. In this case more comprehensive data are needed to increase the feature learning and extraction and produce a model with higher prediction accuracy. Collecting data for various distresses and types of pavements and using techniques such as LIDAR or multispectral camera and creating 3D models for pavement distresses will aid in more realistic and improved evaluation of the pavement distresses, along with quantifying the pavement damage. Additionally, expanding the research to a road network level and geo-referencing the aerial image will provide exact record of the roadways and location of the distresses which may enable emergency responders locating the safe routes for relief, especially after natural hazards.

Development of image segmentation model for quantification of the percentage of pavement distress will aid in decision making regarding immediate repair and maintenance. Additionally, development of Graphical User Interfaces (GUIs) or application-based interface will ease the adoption of these methods to rapidly assess pavement conditions.

## REFERENCES

- Abdeljaber, O., Avci, O., Kiranyaz, M. S., Boashash, B., Sodano, H., & Inman, D. J. (2018). 1-D CNNs for structural damage detection: Verification on a structural health monitoring benchmark data. *Neurocomputing*, 275, 1308-1317. doi:<https://doi.org/10.1016/j.neucom.2017.09.069>
- Adams, S., Friedland, C., & Levitan, M. (2010). *Unmanned aerial vehicle data acquisition for damage assessment in hurricane events*. Paper presented at the Proceedings of the 8th International Workshop on Remote Sensing for Disaster Management, Tokyo, Japan.
- Aksamit, P., & Szmechta, M. (2011). *Distributed, mobile, social system for road surface defects detection*. Paper presented at the 2011 5th International Symposium on Computational Intelligence and Intelligent Informatics (ISCII), Floriana, Malta.
- Ashour, R., Taha, T., Mohamed, F., Hableel, E., Kheil, Y. A., Elsalamouny, M., Kadadha, M., Rangan, K., Dias, J., & Seneviratne, L. (2016). *Site inspection drone: A solution for inspecting and regulating construction sites*. Paper presented at the 2016 IEEE 59th International Midwest Symposium on Circuits and Systems (MWSCAS), Abu Dhabi, United Arab Emirates.
- Attoh-Okine, N., & Adarkwa, O. (2013). *Pavement condition surveys—overview of current practices*. Retrieved from
- Branco, L. H. C., & Segantine, P. C. L. (2015). MaNIAC-UAV-a methodology for automatic pavement defects detection using images obtained by Unmanned Aerial Vehicles. *Journal of Physics: Conference Series*, 633(1), 012122. doi:<https://doi.org/10.1088/1742-6596/633/1/012122>
- Cafiso, S., Di Graziano, A., & Battiato, S. (2006). *Evaluation of pavement surface distress using digital image collection and analysis*. Paper presented at the Seventh International congress on advances in civil Engineering, Istanbul, Turkey
- Canis, B. (2015). Unmanned aircraft systems (UAS): Commercial outlook for a new industry. In: Congressional Research Service Washington, DC.
- Coenen, T. B., & Golroo, A. (2017). A review on automated pavement distress detection methods. *Cogent Engineering*, 4(1), 1374822. doi:<https://doi.org/10.1080/23311916.2017.1374822>
- Deng, L. (2014). A tutorial survey of architectures, algorithms, and applications for deep learning. *APSIPA Transactions on Signal and Information Processing*, 3. doi:<https://doi.org/10.1017/atsip.2013.9>
- DroneDeploy. (2018). Drones Raise the Bar for Roadway Pavement Inspection. Retrieved from <https://blog.dronedeploy.com/drones-raise-the-bar-for-roadway-pavement-inspection-9c0079465772>

- Ellenberg, A., Branco, L., Krick, A., Bartoli, I., & Kontsos, A. (2014). Use of unmanned aerial vehicle for quantitative infrastructure evaluation. *Journal of Infrastructure Systems*, 21(3), 04014054. doi:[https://doi.org/10.1061/\(ASCE\)IS.1943-555X.0000246](https://doi.org/10.1061/(ASCE)IS.1943-555X.0000246)
- Erdelj, M., Natalizio, E., Chowdhury, K. R., & Akyildiz, I. F. (2017). Help from the sky: Leveraging UAVs for disaster management. *IEEE Pervasive Computing*, 16(1), 24-32. doi:10.1109/MPRV.2017.11
- Ersoz, A. B., Pekcan, O., & Teke, T. (2017). Crack identification for rigid pavements using unmanned aerial vehicles. *IOP Conference Series: Materials Science and Engineering*, 236(1), 012101. doi:<https://doi.org/10.1088/1757-899X/236/1/012101>
- Estrada, M. A. R., & Ndoma, A. (2019). The uses of unmanned aerial vehicles–UAV’s–(or drones) in social logistic: Natural disasters response and humanitarian relief aid. *Procedia Computer Science*, 149, 375-383. doi:<https://doi.org/10.1016/j.procs.2019.01.151>
- Ezequiel, C. A. F., Cua, M., Libatique, N. C., Tangonan, G. L., Alampay, R., Labuguen, R. T., Favila, C. M., Honrado, J. L. E., Canos, V., & Devaney, C. (2014). *UAV aerial imaging applications for post-disaster assessment, environmental management and infrastructure development*. Paper presented at the 2014 International Conference on Unmanned Aircraft Systems (ICUAS), Orlando, FL, USA.
- Floreano, D., & Wood, R. J. (2015). Science, technology and the future of small autonomous drones. *Nature*, 521(7553), 460-466. doi:10.1038/nature14542
- Gopalakrishnan, K., Gholami, H., Vidyadharan, A., Choudhary, A., & Agrawal, A. (2018). Crack damage detection in unmanned aerial vehicle images of civil infrastructure using pre-trained deep learning model. *International Journal for Traffic and Transport Engineering*, 8(1), 1-14. doi:[http://dx.doi.org/10.7708/ijtte.2018.8\(1\).01](http://dx.doi.org/10.7708/ijtte.2018.8(1).01)
- Gopalakrishnan, K., Khaitan, S. K., Choudhary, A., & Agrawal, A. (2017). Deep convolutional neural networks with transfer learning for computer vision-based data-driven pavement distress detection. *Construction and Building Materials*, 157, 322-330. doi:<https://doi.org/10.1016/j.conbuildmat.2017.09.110>
- Guo, Y., Liu, Y., Oerlemans, A., Lao, S., Wu, S., & Lew, M. S. (2016). Deep learning for visual understanding: A review. *Neurocomputing*, 187, 27-48. doi:<https://doi.org/10.1016/j.neucom.2015.09.116Get>
- Hallermann, N., & Morgenthal, G. (2013). *Unmanned aerial vehicles (UAV) for the assessment of existing structures*. Paper presented at the IABSE Symposium Report, Rooterdam, Netherlands.
- Hallermann, N., & Morgenthal, G. (2014). *Visual inspection strategies for large bridges using Unmanned Aerial Vehicles (UAV)*. Paper presented at the Proc. of 7th IABMAS,

International Conference on Bridge Maintenance, Safety and Management, Shanghai, China.

- Helali, K., Robson, M., Nicholson, R., & Bekheet, W. (2008). *Importance of a pavement management system in assessing pavement damage from natural disasters: a case study to assess the damage from Hurricanes Katrina and Rita in Jefferson Parish, Louisiana*. Paper presented at the 7th International Conference on Managing Pavement Assets, Calgary, Alberta, Canada.
- High, D. R., Cantrell, R. L., & O'brien, J. J. (2019). System and method for operating drones under micro-weather conditions. In: Google Patents.
- Hinton, G. E., Srivastava, N., Krizhevsky, A., Sutskever, I., & Salakhutdinov, R. R. (2012). Improving neural networks by preventing co-adaptation of feature detectors. *arXiv preprint arXiv:1207.0580*. doi:<https://arxiv.org/abs/1207.0580>
- Ibragimov, E., Lee, H.-J., Lee, J.-J., & Kim, N. (2020). Automated pavement distress detection using region based convolutional neural networks. *International Journal of Pavement Engineering*, 1-12. doi:<https://doi.org/10.1080/10298436.2020.1833204>
- Inzerillo, L., Di Mino, G., & Roberts, R. (2018). Image-based 3D reconstruction using traditional and UAV datasets for analysis of road pavement distress. *Automation in Construction*, 96, 457-469. doi:<https://doi.org/10.1016/j.autcon.2018.10.010>
- Jordan, S., Moore, J., Hovet, S., Box, J., Perry, J., Kirsche, K., Lewis, D., & Tse, Z. T. H. (2018). State-of-the-art technologies for UAV inspections. *IET Radar, Sonar & Navigation*, 12(2), 151-164. doi:10.1049/iet-rsn.2017.0251
- Karim, F. M., Rubasi, K. A. H., & Saleh, A. A. (2016). The road pavement condition index (PCI) evaluation and maintenance: a case study of Yemen. *Organization, Technology and Management in Construction: an International Journal*, 8(1), 1446-1455. doi:10.1515/otmcj-2016-0008
- Khan, F., Ellenberg, A., Mazzotti, M., Kontsos, A., Moon, F., Pradhan, A., & Bartoli, I. (2015). *Investigation on bridge assessment using unmanned aerial systems*. Paper presented at the Structures Congress 2015, Portland, Oregon.
- Kim, I.-H., Jeon, H., Baek, S.-C., Hong, W.-H., & Jung, H.-J. (2018). Application of crack identification techniques for an aging concrete bridge inspection using an unmanned aerial vehicle. *Sensors*, 18(6), 1881. doi: <https://doi.org/10.3390/s18061881>
- Krizhevsky, A., Sutskever, I., & Hinton, G. E. (2012). *Imagenet classification with deep convolutional neural networks*. Paper presented at the Advances in neural information processing systems, Shenyang, China.

- Lekshmiopathy, J., Samuel, N. M., & Velayudhan, S. (2020). Vibration vs. vision: best approach for automated pavement distress detection. *International Journal of Pavement Research and Technology*, 1-9. doi:<https://doi.org/10.1007/s42947-020-0302-y>
- Li, S., & Zhao, X. (2019). Image-Based Concrete Crack Detection Using Convolutional Neural Network and Exhaustive Search Technique. *Advances in Civil Engineering*, 2019. doi:<https://doi.org/10.1155/2019/6520620>
- Li, Y., & Liu, C. (2019). Applications of multirotor drone technologies in construction management. *International Journal of Construction Management*, 19(5), 401-412. doi:<https://doi.org/10.1080/15623599.2018.1452101>
- Li, Z., Cheng, C., Kwan, M.-P., Tong, X., & Tian, S. (2019). Identifying asphalt pavement distress using UAV LiDAR point cloud data and random forest classification. *ISPRS International Journal of Geo-Information*, 8(1), 39. doi:<https://doi.org/10.3390/ijgi8010039>
- Lindell, M. K., & Prater, C. S. (2003). Assessing Community Impacts of Natural Disasters. *Natural Hazards Review*, 4(4), 176-185. doi:10.1061/(ASCE)1527-6988(2003)4:4(176)
- Liu, P., Chen, A. Y., Huang, Y.-N., Han, J.-Y., Lai, J.-S., Kang, S.-C., Wu, T.-H., Wen, M.-C., & Tsai, M.-H. (2014). A review of rotorcraft unmanned aerial vehicle (UAV) developments and applications in civil engineering. *Smart Struct. Syst*, 13(6), 1065-1094. doi:<http://dx.doi.org/10.12989/sss.2014.13.6.1065>
- Luppigini, R., & So, A. (2016). A technoethical review of commercial drone use in the context of governance, ethics, and privacy. *Technology in Society*, 46, 109-119. doi:<https://doi.org/10.1016/j.techsoc.2016.03.003>
- Miller, J. S., & Bellinger, W. Y. (2003). *Distress identification manual for the long-term pavement performance program*. Retrieved from
- Morton, M., & Levy, J. L. (2011). Challenges in disaster data collection during recent disasters. *Prehospital and disaster medicine*, 26(3), 196-201. doi:10.1017/S1049023X11006339
- Nair, V., & Hinton, G. E. (2010). *Rectified linear units improve restricted boltzmann machines*. Paper presented at the ICML, Haifa, Israel.
- Nasir, N. H. M., Mohamed, W. M. W., & Tahar, K. N. (2018). A Review on Road Distress Detection Methods. *Advances in Transportation and Logistics Research*, 1, 230-241. doi:<https://doi.org/10.25292/atlr.v1i1.28>
- Nedjati, A., Vizvari, B., & Izbirak, G. (2016). Post-earthquake response by small UAV helicopters. *Natural Hazards*, 80(3), 1669-1688. doi:10.1007/s11069-015-2046-6

- Nie, M., & Wang, K. (2018). *Pavement distress detection based on transfer learning*. Paper presented at the 2018 5th International Conference on Systems and Informatics (ICSAI), Nanjing, China.
- Oliveira, H., & Correia, P. L. (2014). *CrackIT—An image processing toolbox for crack detection and characterization*. Paper presented at the 2014 IEEE international conference on image processing (ICIP), Paris, France.
- Pan, Y., Zhang, X., Cervone, G., & Yang, L. (2018). Detection of asphalt pavement potholes and cracks based on the unmanned aerial vehicle multispectral imagery. *IEEE Journal of Selected Topics in Applied Earth Observations and Remote Sensing*, 11(10), 3701-3712. doi:10.1109/JSTARS.2018.2865528
- Pierce, L. M., McGovern, G., & Zimmerman, K. A. (2013). *Practical guide for quality management of pavement condition data collection*.
- Ragnoli, A., De Blasiis, M. R., & Di Benedetto, A. (2018). Pavement distress detection methods: A review. *Infrastructures*, 3(4), 58. doi:<https://doi.org/10.3390/infrastructures3040058>
- Rao, B., Gopi, A. G., & Maione, R. (2016). The societal impact of commercial drones. *Technology in Society*, 45, 83-90. doi:<https://doi.org/10.1016/j.techsoc.2016.02.009>
- Rashid, Z. B., & Gupta, R. (2017). Study of Defects in Flexible Pavement and its Maintenance. *International Journal of Recent Engineering Research and Development*, 2(6), 74-77.
- Restas, A. (2015). Drone applications for supporting disaster management. *World Journal of Engineering and Technology*, 3(03), 316. doi:10.4236/wjet.2015.33C047
- Saad, A. M., & Tahar, K. N. (2019). Identification of rut and pothole by using multirotor unmanned aerial vehicle (UAV). *Measurement*, 137, 647-654. doi:<https://doi.org/10.1016/j.measurement.2019.01.093>
- Sankarasrinivasan, S., Balasubramanian, E., Karthik, K., Chandrasekar, U., & Gupta, R. (2015). Health monitoring of civil structures with integrated UAV and image processing system. *Procedia Computer Science*, 54, 508-515. doi:<https://doi.org/10.1016/j.procs.2015.06.058>
- Schnebele, E., Tanyu, B., Cervone, G., & Waters, N. (2015). Review of remote sensing methodologies for pavement management and assessment. *European Transport Research Review*, 7(2), 7. doi:10.1007/s12544-015-0156-6
- Shiyab, A. M. (2007). *Optimum use of the flexible pavement condition indicators in pavement management system*. Curtin University,
- Srivastava, N., Hinton, G., Krizhevsky, A., Sutskever, I., & Salakhutdinov, R. (2014). Dropout: a simple way to prevent neural networks from overfitting. *The journal of machine learning research*, 15(1), 1929-1958.

- Tanner, V. (2018). *Using Drones in Disaster Areas: Perspectives of Disaster Responders in North Carolina, Virginia and Maryland*.
- Tanzi, T. J., Chandra, M., Isnard, J., Camara, D., Sebastien, O., & Harivelo, F. (2016). *Towards "drone-borne" disaster management: future application scenarios*. Paper presented at the XXIII ISPRS Congress, Commission VIII (Volume III-8), Prague, Czech Republic.
- Tatum, M. C., & Liu, J. (2017). *Unmanned aerial vehicles in the construction industry*. Paper presented at the Proceedings of the Unmanned Aircraft System Applications in Construction, Creative Construction Conference, Primosten, Croatia.
- Tighe, S. L., Ningyuan, L., & Kazmierowski, T. (2008). Evaluation of semiautomated and automated pavement distress collection for network-level pavement management. *Transportation Research Record*, 2084(1), 11-17. doi:<https://doi.org/10.3141/2084-02>
- Wang, W., Wu, B., Yang, S., & Wang, Z. (2018). *Road damage detection and classification with Faster R-CNN*. Paper presented at the 2018 IEEE International Conference on Big Data (Big Data), Seattle, WA, USA.
- Wang, X., & Hu, Z. (2017). *Grid-based pavement crack analysis using deep learning*. Paper presented at the 2017 4th International Conference on Transportation Information and Safety (ICTIS), Banff, AB, Canada.
- Weinmann, T. L., Lewis, A. E., & Tayabji, S. (2004). *Pavement sensors used at accelerated pavement test facilities*. Paper presented at the Proceedings of the second international conference on accelerated pavement testing, Minneapolis, MN, USA.
- Wells, J. L., Lovelace, B., & Kalar, T. (2017). Use of unmanned aircraft systems for bridge inspections. *Transportation Research Record*, 2612(1), 60-66. doi:<https://doi.org/10.3141/2612-07>
- Xie, D., Zhang, L., & Bai, L. (2017). Deep learning in visual computing and signal processing. *Applied Computational Intelligence and Soft Computing*, 2017. doi:<https://doi.org/10.1155/2017/1320780>
- Yokoyama, S., & Matsumoto, T. (2017). Development of an automatic detector of cracks in concrete using machine learning. *Procedia engineering*, 171, 1250-1255. doi:<https://doi.org/10.1016/j.proeng.2017.01.418>
- Zakeri, H., Nejad, F. M., & Fahimifar, A. (2016). Rahbin: A quadcopter unmanned aerial vehicle based on a systematic image processing approach toward an automated asphalt pavement inspection. *Automation in Construction*, 72, 211-235. doi:<https://doi.org/10.1016/j.autcon.2016.09.002>

- Zakeri, H., Nejad, F. M., & Fahimifar, A. (2017). Image based techniques for crack detection, classification and quantification in asphalt pavement: a review. *Archives of Computational Methods in Engineering*, 24(4), 935-977. doi:10.1007/s11831-016-9194-z
- Zhang, C. (2008). An UAV-based photogrammetric mapping system for road condition assessment. *Int. Arch. Photogramm. Remote Sens. Spatial Inf. Sci*, 37, 627-632. doi:10.1.1.150.8490&rep=rep1&type=pdf
- Zhang, C., & Elaksher, A. (2012). An Unmanned Aerial Vehicle-Based Imaging System for 3D Measurement of Unpaved Road Surface Distresses. *Computer-Aided Civil and Infrastructure Engineering*, 27(2), 118-129. doi: <https://doi.org/10.1111/j.1467-8667.2011.00727.x>

## APPENDIX

### Flexible Pavement Distresses

**1. Cracking:** It is a consequence of the climatic conditions and traffic loading and includes the following subdivisions: alligator cracking, block cracking, edge cracking, longitudinal cracking, reflection cracking, and transverse cracking. These subdivisions are distinguished and identified based on the size, form, characteristics, and orientation of their appearance. Their appearance impact the comfort and safety of pavement operation, and at times the forth coming end of the pavement life-cycle (Ragnoli et al., 2018).

1.1 Alligator cracking: It is also known as fatigue cracking which occurs in the form of a series of interconnected cracks, a pattern resembling the skin of an alligator. These cracks result from repeated traffic loading (fatigue failure) forming many-sided and sharp-angled pieces with the longest side usually measuring up to 0.3 m or 1 foot. The severity of these cracks is identified as low, moderate, or high based on the area covered by the cracks (Miller et al., 2003; Rashid et al., 2017).



Figure A1: Alligator Cracking in Flexible Pavements

1.2 Block cracking: It occurs in the pattern of interconnected square or rectangular blocks on the surface of the pavement. These blocks are usually in the size range of 0.1 to 10 m<sup>2</sup> extending over a large part of the pavement surface area. The cracked area is measured in order to determine the severity of the cracking (Miller et al., 2003; Pierce et al., 2013; Rashid et al., 2017).



Figure A2: Block Cracking in Flexible Pavements

1.3 Edge Cracking: It occurs along the edges of the pavement surface as a result of poor drainage and lack of appropriate support at the pavement edges. Continuous or crescent shaped cracks intersecting the pavement edges are formed at the edge of pavement alongside the shoulder usually within 0.6 m (Miller et al., 2003).



Figure A3: Edge Cracking in Flexible Pavements

1.4 Longitudinal Cracking: It occurs along the centerline of the pavement. Depending on the location at which it appears in the lane, it can either be the wheel path or non-wheel path. Longitudinal cracks ultimately develop into alligator cracks under repeated traffic loading. The severity of these cracks is identified as low, moderate, or high based on the linear measurement of the cracks. (Miller et al., 2003; Rashid et al., 2017).



Figure A4: Longitudinal Cracking in Flexible Pavements

1.5 Reflection Cracking: It occurs in the flexible overlays of concrete pavements over the joints due to the joint movement. Reflective cracks also appear in asphalt pavements over other cracks or pavements with a stabilized base.



Figure A5: Reflection Cracking in Flexible Pavements

1.6 Transverse Cracking: It occurs along the width or perpendicular to the centerline of the pavement. It is caused by hardening of asphalt binder or the shrinkage of the surface layer due to low temperatures (Miller et al., 2003).



Figure A6: Transverse Cracking in Flexible Pavements

**2. Patching and Potholes:** Patching is replacement of the part of or an area of the existing pavement with new material to repair the pavement surface deterioration usually greater than or equal to 0.1 m<sup>2</sup> (Figure A7a). The patches are more or less same as the original pavement in terms of quality and their addition of patches impacts the driving safety and comfort, especially when the patches start to deteriorate. Potholes are bowl-shaped holes of differing sizes on the surface of the pavement and sometimes extending all the way to the base course (Figure A7b). The minimum plan dimension for a pothole is 150 mm in diameter (Coenen et al., 2017; Miller et al., 2003).

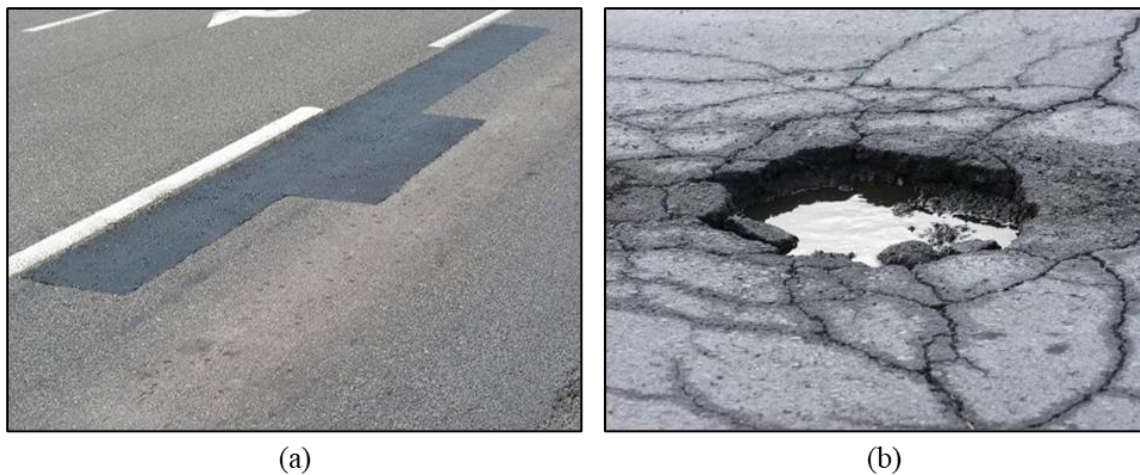


Figure A7: Patching (a) and Potholes (b) in Flexible Pavements

**3. Surface Deformation:** This distress group includes rutting and shoving as its sub-categories. It occurs due to the horizontal and vertical dislocation and localization of surface layer. The longitudinal depression of the of the pavement surface along the wheel path is called rutting (Figure A8a), whereas shoving results from the longitudinal displacement or a localized bulging of the pavement surface in the form of hills or curves occurring at sharp curves or at points of accelerating and breaking traffic (Figure A8b) (Coenen et al., 2017; Miller et al., 2003; Rashid et al., 2017).

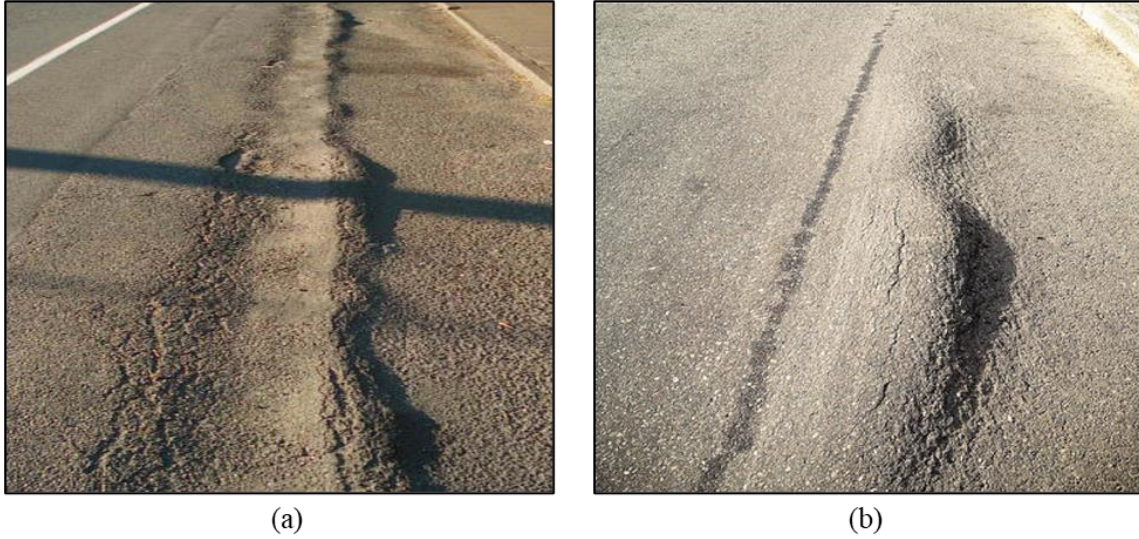


Figure A8: Surface Defects; Rutting (a) and Shoving (b) in Flexible Pavements

- 4. Surface Defects:** Surface defects are a result of the deteriorating surface layer of the pavement due to traffic and the material characteristics of the surface layer. These incorporate bleeding, polished aggregate and raveling. Bleeding is a consequence of the excess asphalt binder, encountered as a discoloration on the pavement surface as compared to the rest of the pavement, generally found in the wheel paths (Figure A9a). Polished aggregate is the exposure of the coarse aggregate on the pavement surface caused by the wearing of the surface binder and decreased adhesion resulting in a smooth surface layer and reduced skid resistance (Figure A9b). Raveling occurs when the aggregate particles in the pavement surface are dislodged because of loss of surface binder and reduced adhesion (Figure A9c) (Coenen et al., 2017; Miller et al., 2003; Ragnoli et al., 2018).

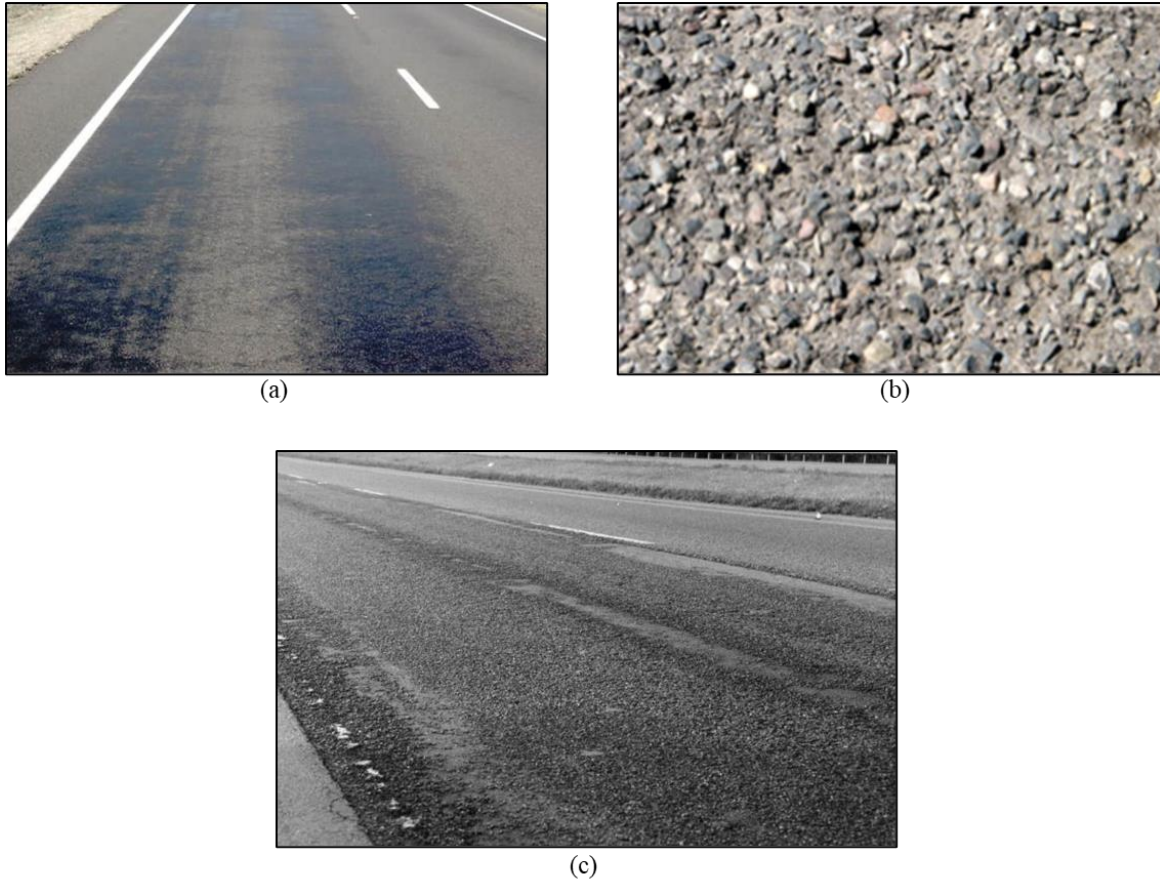


Figure A9: Surface Deformations; Bleeding (a), Polished Aggregate (b), and Raveling (c) in Flexible Pavements

**5. Miscellaneous Distresses:** These include lane-to-shoulder dropoff and water bleeding and pumping. The lane-to-shoulder dropoff is also called edge dropoff is a result of the difference in elevation between the traveled surface and the outside shoulder due to the settlement of the shoulder because of lack of subgrade support (Figure A10a). Water bleeding and pumping occurs when the water beneath the pavement either seeps or is discharged through the joints and cracks, typically encountered on the surface through deposits of water and fine material eroded from the underlying layers of the pavement (Figure A10b) (Coenen et al., 2017; Miller et al., 2003).



(a)



(b)

Figure A10: Miscellaneous Distresses; Lane-to-Shoulder Dropoff (a) and Water Bleeding and Pumping in Flexible Pavements

## Rigid Pavement Distresses

**1. Cracking:** Cracking on rigid pavements include corner breaks, durability “D” cracking, longitudinal cracking, and transverse cracking.

1.1 Corner Breaks: They occur as a result of high corner stresses in concrete pavements. These extend from the corners of the pavement intersecting the adjacent transverse and longitudinal joints at an angle of approximately  $45^\circ$  widthwise (Figure A11). Their length measures from 0.3 m to half the size of the width of the pavement (Miller et al., 2003).



Figure A11: Corner Breaks in Rigid Pavements

1.2 Durability “D” Cracking: It occurs in the form of closely spaced, crescent-shaped cracks due to the contraction and expansion of the large aggregate within the pavement. It usually initiates from slab corners and appears near the joints, cracks, or free edges of the pavements in a hairline cracking pattern (Figure A12). (Miller et al., 2003).



Figure A12: Durability “D” Cracking in Rigid Pavements

1.3 Longitudinal Cracking: It is similar to the flexible pavements. The cracks appear primarily in the direction of the traffic, along the centerline of the pavement (Figure A13). The severity of the cracks is determined based on the width of the cracks and the corresponding spalling (Miller et al., 2003).



Figure A13: Longitudinal Cracking in Rigid Pavements

1.4 Transverse Cracking: It appears in the similar manner as flexible pavements. The cracks occur widthwise adjacent to the joints, perpendicular to the centerline of the pavement (Figure A14).

Like longitudinal cracks in rigid pavements, the severity of the cracks is determined based on the width of the cracks and the corresponding spalling (Miller et al., 2003).



Figure A14: Transverse Cracking in Rigid Pavements

**2. Joint Deficiencies:** This includes joint seal damage (transverse and longitudinal), spalling of longitudinal joints, and spalling of transverse joints.

2.1 Joint Seal Damage: It occurs due to the infiltration of water or incompressible material through the pavement joints from the surface. It can appear in both longitudinal and transverse joints and includes extrusion, hardening, adhesive failure (bonding), cohesive failure (splitting), complete loss of sealant, intrusion of foreign material into the joint or grass or weed growth in the joint (Figure A15) (Miller et al., 2003).



Figure A15: Joint Seal Damage in Rigid Pavements

2.1 Spalling of Longitudinal Joints: It refers to the cracks or breaks on the surface of the pavement at longitudinal joints. It may also occur as chipping or fraying of pavement edges usually within 0.3 m from the face of the longitudinal joint (Figure A16) (Miller et al., 2003).



Figure A16: Spalling of Longitudinal Joints in Rigid Pavements

2.3 Spalling of Transverse Joints: It is identical to the spalling of longitudinal joints except it occurs along laterally appearing as cracks or breaks on the surface of the pavement along the transverse joints. It may also occur as chipping or fraying of pavement edges usually within 0.3 m from the face of the transverse joint (Figure A17) (Miller et al., 2003).



Figure A17: Spalling of Transverse Joints in Rigid Pavements

**3. Surface Defects:** appear on the surface layer of rigid pavements and include map cracking and scaling, polished aggregate, and popouts.

3.1 Map Cracking and Scaling: Map Cracking appears as a series of interconnected cracks on the surface of the pavement, usually longer in length in the longitudinal direction along with smaller or finer cracks in the transverse or random cracks (Figure A18a). Scaling occurs in the form of deterioration of the upper surface of the pavement usually 3 to 13 mm (Figure A18b) (Miller et al., 2003).



(a)



(b)

Figure A18: Map Cracking (a) and Scaling (b) in Rigid Pavements

3.2 Polished Aggregate: It is the exposure of coarse aggregate on the surface of the pavement due to loss of surface mortar and texturing (Figure A19). It results in decreased skid resistance or surface friction of pavements (Miller et al., 2003).



Figure A19: Polished Aggregate in Rigid Pavements

3.3 Popouts: They occur due to surface material being broken loose into small pieces leaving empty pockets on the surface of the pavement (Figure A20). These usually range from 25 to 100 mm in diameter and 13 to 50 mm in depth (Miller et al., 2003).



Figure A20: Popouts in Rigid Pavements

**4. Miscellaneous Distresses:** Miscellaneous distresses for rigid pavements include blowups, faulting of transverse joints and cracks, lane-to-shoulder dropoff, lane-to-shoulder separation, patch/patch deterioration, and water bleeding and pumping.

4.1 Blowup: It occurs due to the insufficient room for expansion of the slab during hot weather seasons in the form of a localized upward movement of pavement surface at the transverse joints, consequently, the concrete is shattered in that area (Figure A21) (Miller et al., 2003).



Figure A21: Blowups in Rigid Pavements

4.2 Faulting of Transverse Joints and Cracks: It occurs as a result of the difference in elevation across a joint or a slab due to slab pumping, settlement, curling or warping (Figure A22) (Miller et al., 2003).



Figure A22: Faulting of Transverse Joints and Cracks in Rigid Pavements

4.3 Lane-to-Shoulder Dropoff: It is identical to flexible pavements and occurs due to the difference in elevation between the edge of the slab and the outside shoulder because of the settlement of the shoulder (Figure A23) (Miller et al., 2003).



Figure A23: Lane-to-Shoulder Dropoff in Rigid Pavements

4.4 Lane-to-Shoulder Separation: It occurs when the joint between the edge of the slab and the adjacent shoulder widens (Figure A24) (Miller et al., 2003).



Figure A24: Lane-to-Shoulder Separation in Rigid Pavements

4.5 Patch/Patch Deterioration: Patching refers to a part of the existing pavement being replaced by new or additional material to repair the pavement surface deterioration usually greater than or equal to 0.1 m<sup>2</sup> (Figure A25). Patch deterioration refers to the degradation of the replaced patch of the pavement (Miller et al., 2003).

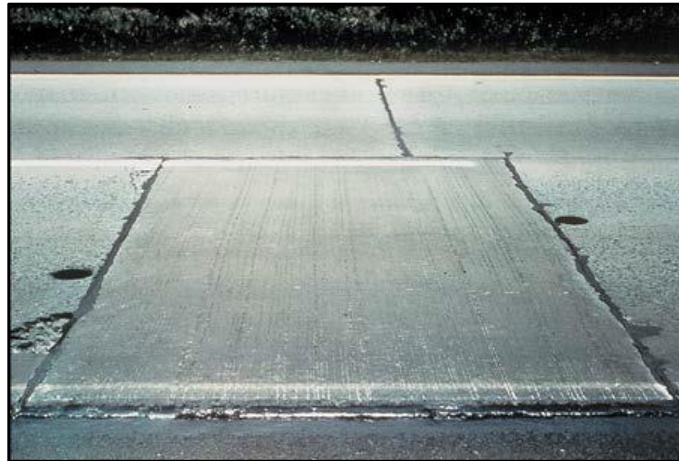


Figure A25: Patching in Flexible Pavements

4.6 Water Bleeding and Pumping : occur similar to the flexible pavements where the water beneath the pavement either seeps or is discharged through the joints and cracks, typically encountered on the surface through deposits of water and fine material eroded from the underlying layers of the pavement (Figure A26) (Miller et al., 2003).



Figure A26: Water Bleeding and Pumping in Rigid Pavements

